Journal of Intelligent Machinery Equipment

MASON PUBLISH GROUP

Journal of Intelligent Machinery and Equipment

DISCLAIMER

The Publisher, Associations and Editors cannot be held responsible for errors or any consequences arising from the use of information contained in this journal; the views and opinions expressed do not necessarily reflect those of the Publisher, Associations and Editors.

Editorial Team

Publication Ethics and Malpractice Statement

The *Journal of Intelligent Machinery and Equipment* is an academic journal published by Mason Publish Group. It is necessary to agree upon standards of expected ethical behavior for all parties involved in the act of publishing: the journal editor, the author, the peer reviewer and the publisher. This ethic statement is based on COPE's Best Practice Guidelines for Journal Editors.

Duties of Editor

- The evaluation should be objective and fair, and give clear opinions on whether it meets the standards of public publication.
- Ensure that journals are published on time and on schedule, and prevent plagiarism and repeated publication of papers.
- According to the importance, originality and relevance of the paper to the journal, the author has the right to reject and accept the paper, and allows the author to appeal the review decision.
- The editor shall ensure that all research material they publish conforms to internationally accepted ethical guidelines.

Duties of Authors

- Authors have to make sure that they write completely original works that have not been published elsewhere before.
- The data of the paper is authentic and reliable, and forgery, tampering and plagiarism are prohibited.
- Reference information shall be indicated when quoting opinions.
- The author shall ensure that the published paper is authorized and approved by the coauthor, and there is no signed dispute.
- All authors must contribute to the research of the paper.
- The author shall provide the original data related to his manuscript for the editor's review, and must keep these data.

Duties of Reviewers

In the process of review, the reviewer shall be objective and keep all information of the paper confidential. Reviewers must ensure that the author has identified all data sources used in the study. If invited to review a paper, it shall be completed within the specified time.

Duties of Advisory Board Members

The advisory board is composed of distinguished scholars and professors in the field of Journal of Intelligent Machinery and Equipment. Members can review submitted manuscripts, identify topics for special issues, or attract new authors and submissions as necessary.

Journal of Intelligent Machinery and Equipment

Call for Papers

We rapid evolution brings urgent ethical and legal challenges, from algorithmic fairness to regulatory frameworks. Journal of Intelligent Machinery and Equipment (Mason Publish Group, peer-reviewed) invites global researchers, scholars, and practitioners to contribute original works on AI's machinery and equipment intersections.We welcome original research, case studies, and theoretical explorations linking AI technology, machinery, and equipment. Join us in shaping responsible AI development and fostering global dialogue in this critical field.

Call for Reviewers

In order to further improve the academic level and quality of the journal, enrich the team of reviewers and implement the anonymous reviewer system, the editorial department is now calling for reviewers. We welcome experts and scholars in the fields of the Journal of Intelligent Machinery and Equipment to recommend themselves or recommend suitable candidates, so as to jointly promote the progress and development of periodicals. Please contact us (editorialoffice@masonpublish.org) if you are interested.

Journal of Intelligent Machinery and Equipment

Articles

Study on Microstructure and Properties of the Additive Layer of FCW Wire for H13 Steel

Xinhua Xiao*

University Science Park, Hubei Institute of Technology University Science and Technology, Huangshi 435003, Hubei, China

*Corresponding author, E-mail: xiaoxinhua12@126.com

Abstract:

In order to provide research data on direct forming and rapid recovery of metal parts by arc fuse additive manufacturing technology. In this paper, the flux cored wire prepared from H13 die steel strip was used as the wire material, and the arc additive manufacturing process was used to carry out multi-channel and multi-layer surfacing welding process test on the Cr12MoV steel substrate, and the quality, structure and performance of the additive layer were studied. The results show that there is obvious fusion line between layers, and there is no porosity, crack or unfusion in the section. The average interlayer microhardness was 325HV, slightly higher than that of annealed substrate. The change pattern of microstructure from bottom to top layer is from equiaxed crystal to larger equiaxed crystal. The top layer is columnar crystal, and the microstructure is mixed structure of martensite, alloy compound and bainite. The tensile test showed that the tensile strength between layers was about 700Mpa, with no obvious yield strength and the elongation reaching 11.9%.The wear test shows that the additive layer has better wear resistance, and wear is a mixture mechanism of abrasive wear and adhesive wear. H13 steel flux-cored wire is suitable for direct manufacture of wear - resistant parts and mold repair.

Keywords:

Arc fuse additive manufacturing，Mold repair，Mechanical properties，Friction and wear

1 Introduction

In the mould manufacturing industry, moulds are subjected to large stresses and deformations due to their alternating harsh service environments, which ultimately lead to wear and tear, cracks, fractures, and eventual failure. Technological innovation has led to the study of mould remanufacturing technology, and currently, the commonly used repair technologies include thermal spraying, laser cladding technology, electric spark, electric arc surfacing (arc additive manufacturing), and electrobrush plating, etc [1-5]. Among them, arc wire additive manufacturing (WAAM) technology is one of the important research directions in the field of 3D additive manufacturing of metal materials, and the research boom of direct forming metal parts and parts repair by arc wire additive manufacturing technology is being set off at home and abroad. For this reason, this paper selects H13 mould steel with coated alloy powder prepared flux-cored wire as wire material, using arc additive manufacturing technology, multi-channel multi-layer 3D overlay welding of straight-walled parts on the mould steel substrate, to carry out research on the organisation and properties of the mould steel arc additive layer, to provide data support for the development of processes and materials for the remanufacturing of moulds and the direct manufacturing of parts and other aspects.

2 Testing and Analysis

2.1 Research on multi-layer and multi-pass forming process

In the test with the use of argon as a shielding gas, gas flow rate of 16L/min, welding speed of 5mm/s, the distance from the nozzle to the workpiece is 10.5mm, the current is 110A, the voltage is 20V, the flux-cored wire prepared from H13 mould steel strip is used as the wire material, and the arc additive manufacturing technology is used to carry out multi-layer overlays on the Cr12MoV mould steel substrate, and the temperature of the interlayer is controlled at 150 ~ 200℃. Round-trip 4-channel 15-layer high multi-channel multilayer cladding layer, will be obtained after 15 layers of size of about 120mm × 50mm × 8mm arc 3D additive material additive multichannel multilayer vertical wall pieces cut corrosion and polishing, the macroscopic organisation of the photographs obtained as shown in Figure 1: Observation of Figure 1 shows that there are obvious boundaries between the layer and the layer, the thickness of the layer between the fluctuations in the 2.1 ~ 2.3mm, from the macroscopic morphology of the cross-sectional observation of the absence of porosity No air holes, cracks, no unfused and other phenomena, indicating that the arc 3D additive interlayer bonding is good, dense organisation; the measured composition of the molten metal is shown in Table 1.
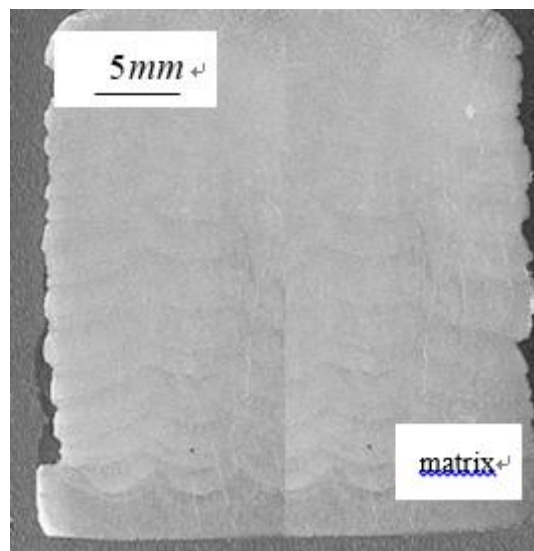
Figure 1: Macroscopic morphology of additive layer

Table 1 Composition of deposited metal (mass percentage)　　　　**%**

C	Ni	Cr	Mo	V	Si	Mn	P	S
0.21~0.32	1.5~1.7	1.9~3.1	0.9~1.1	0.5~0.59	0.3~0.38	1.1~1.21	≤0.03	≤0.03

2.2 Hardness and mechanical properties

2.2.1 Hardness Test

Hardness is an index of the comprehensive mechanical properties of materials. For this reason, the Vickers microhardness test was carried out on the additive layer specimen, and the test results are shown in Figure 2. It can be seen that the average hardness of the arc 3D additive layer of 325HV, in which the hardness value of

the lower part of the vertical wall pieces is slightly lower than the upper part of the hardness value, this is due to the lower layer of the substrate is close to the bottom of the bottom layer of heat dissipation conditions are better than the upper layer of the metal, the microstructure is dense, the compound hard phase is not anxious to gather, the distribution of hardness value is more uniform; the higher the hardness value of the additive is the more on the higher side, this is due to the latter layer of the accumulation of heat, the more carbides gathered grain boundaries, resulting in stress concentration hardness is high. This is due to the accumulation of heat in the latter layer, more carbides gathered at grain boundaries, resulting in high stress concentration hardness. The hardness of the entire additive layer is higher than the substrate (annealed cold work mould steel Cr12MoV microhardness of 310 ~ 257HV), it can be seen, the additive layer of comprehensive mechanical properties.
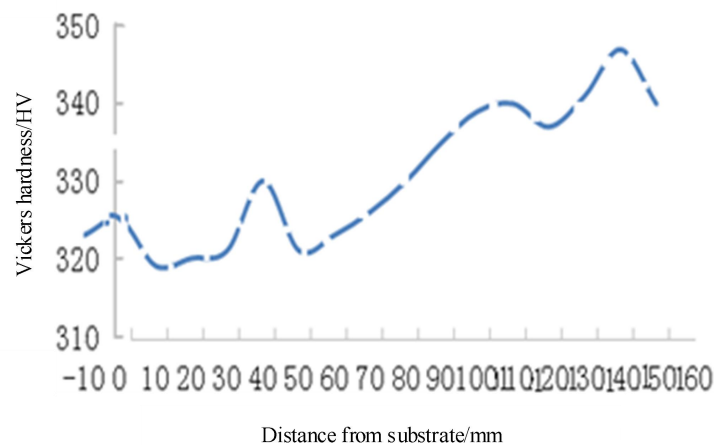
Figure 2: Hardness distribution from the substrate towards the additive layer in the height direction

2.2.2 Tensile test

Use WDW-100 type universal testing machine arc 3D additive material after the addition of single-pass multilayer vertical wall piece specimens for room temperature tensile performance testing, determination of its strength index. According to GB/T 228-2002 'room temperature tensile test methods for metal materials' and GB/T 2652-2008 'weld and molten metal tensile test methods' standard, multi-channel multilayer specimens for wire cutting to produce tensile specimens, tensile specimen size as shown in Figure 3, the sampling location for the incremental layer of the direction of the three different positions, in order to later take the average value of the three tensile experiments in which One curve is shown in Figure 4.
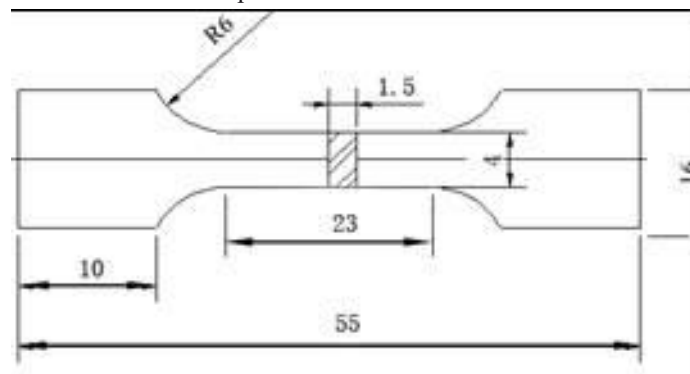
Figure 3: The dimensions of tensile samples
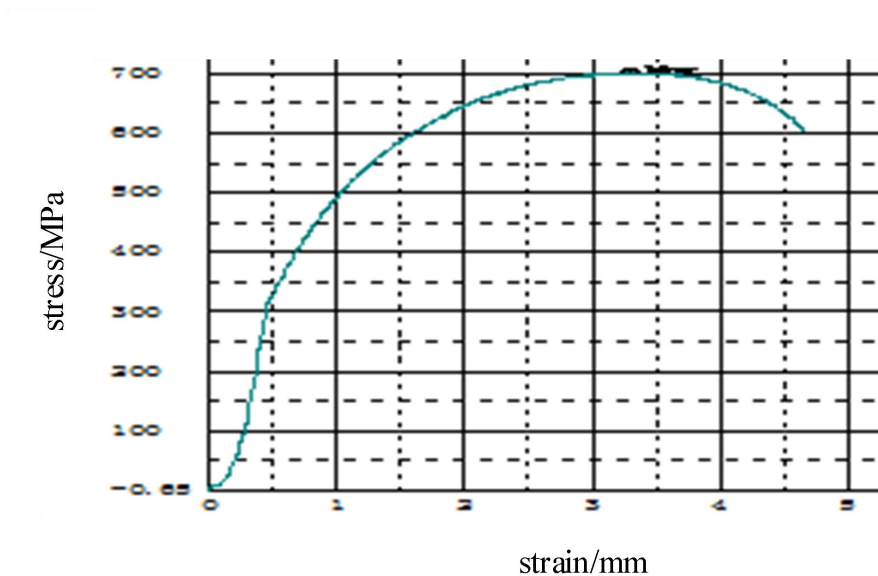
Figure 4: Tensile stress-stroke curve of sedimentary layer

Analysis of the experimental results show that the tensile strength along the augmentation heightening way on the tensile strength of 704.3MPa [(721.2+692.5+700.3)/3] or so, are not obvious yield strength, the conditional yield limit of about 412.4 [(441.2+400.4+395.6)/3] MPa or so, higher than the yield strength of the annealed state rolled Cr12MoV substrate 210 MPa, and the elongation reaches 11.9% [(13.5+10.4+11.9)/3], indicating that the 3D additive interlayer bonding strength is high and the interlayer plasticity is good.

3 Observation of micro-metallographic organisation

The multi-channel multilayer vertical walled parts were sampled for metallographic observation after the arc 3D additive. The metallographic specimens were prepared as follows: firstly, the specimens were cut with a wire cutter with a cutting size of 16mm×16mm×6mm, and then polished with different grits of sandpaper after being smoothed on a SIST-200 grinder, and then polished with a diamond polishing agent with a grit size of 2 μm on a MP-2A metallographic specimen polisher without any scratches; and then corroded with aqua regia (HCL:HNO3=1:3) on the specimens, and cleaned with wine and blown dry for microstructure observation and analysis. The specimen was corroded with aqua regia (HCL:HNO3=1:3), cleaned with wine, blown dry, and then observed and analysed the morphology of microstructure.

As shown in Figure 5, the matrix organisation is dense (shown in 5 (a)), with a clear fusion line between the bottom layer and the matrix, and fine grains (shown in 5 (b)), which benefited from the good heat dissipation conditions of the bottom layer at the initial stage of forming. The trend of heat dissipation conditions in the initial layers is gentle, with little change in grain size from layer to layer (shown in 5(c) (d)); up to the intermediate layer are isometric crystals, except that the grains after the intermediate layer are coarser than those in the matrix and initial layers (shown in 5(g) (h)); the outermost and second outermost layers can be seen as clearly orientated columnar crystalline organisation (shown in 5(i) (j)), due to the accumulation of heat from layer to layer in the process of metal deposition and the directional This is due to the accumulation of heat in the layers during the metal deposition process and the formation of directional heat dissipation conditions, resulting in the generation of coarse columnar crystalline tissue with directionality.
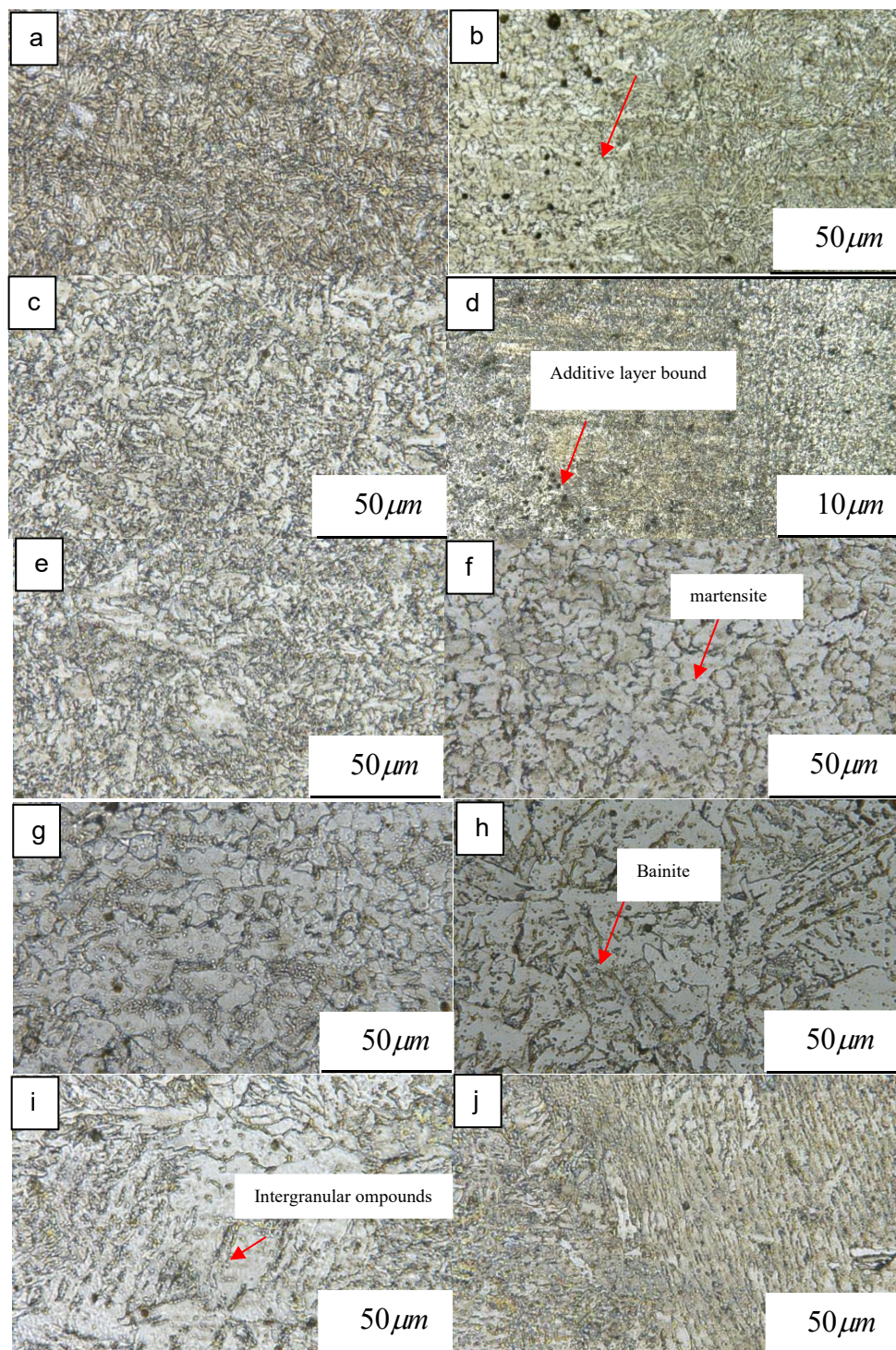
(a) Matrix; (b) Matrix on left, additive layer on right; (c) (d) Between additive layers; (e) First layer; (f) Second layer; (g) Intermediate layer; (h) Sub-intermediate layer; (i) Sub-outer layer; (j) Outer layer

Figure 5:Scanning image of typical layers

4 Wear test

Wear test specimen preparation: the use of wire cutting, along the height of the additive layer to intercept a

pair of specimens, the test parameters are shown in Table 2.

Table 2 Wear testing parameters

Friction parameters	Rotational speed (m/s)	payload (N)	Test duration (min)	counterpart	Friction method	Ambient temperature/humidity
Parameter value	1.09	30	60	Si_3N_4 disc	Rotational motion with dry friction	24°C/65%RH

The coefficient of kinetic friction measured in this specimen is calculated according to the following formula:

$$\eta = \frac{9.45B}{10(A + C) - 2.5B}$$

(1)

where; is the equilibrium load derived from the experiment; is the applied load.

The test results are shown in Figure 6. The friction coefficient increases linearly and rapidly with time delay, from 0.107 to 0.271, and stabilised at 0.359, this is because at the beginning of the test, the surface of the specimen after grinding and processing there is always a certain degree of roughness, there are only a few profile peaks in contact at the beginning, so the friction coefficient rises faster, and the later contact surface is smooth to enter into a steady state, and the friction coefficient basically remains unchanged at the smaller value, which indicates that the additive layer has good abrasion resistance.
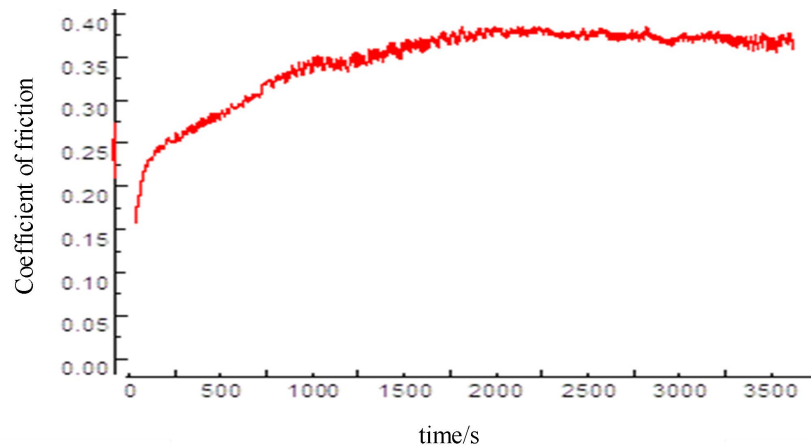
Figure 6: Friction coefficient

Figure 7 shows the results of specimen ESEM experiment. The observed pictures show that there are relatively obvious scratches and surface material flaking on the wear surface, and a large number of white abrasive chips are gathered in the local tissues, and the wear is a mixed mechanism of abrasive grain wear and adhesive wear. This is due to the block shedding and furrowing that occurs in the later stages of wear. The uneven distribution of stresses during the wear process results in the rupture, shedding and aggregation of hard phases, and the formation of furrows as these hard phases move relative to each other in the direction of friction on the soft substrate under the action of inertial forces. For carbon steel materials, the content, type, morphology, and distribution of alloying compounds and carbides Cm have a great influence on the wear

resistance of steel [6-12]. This melting material is rich in V, Cr, Mn for strong carbide formation elements, can promote the formation of carbide hard phase, these hard phase diffuse distribution in the matrix grain boundaries, play the role of nail rolling dislocations, strengthen the role of the matrix, which improves the microhardness of the additive layer, play a wear-resistant skeleton to improve the role of wear resistance in the abrasion test and service imperial process.
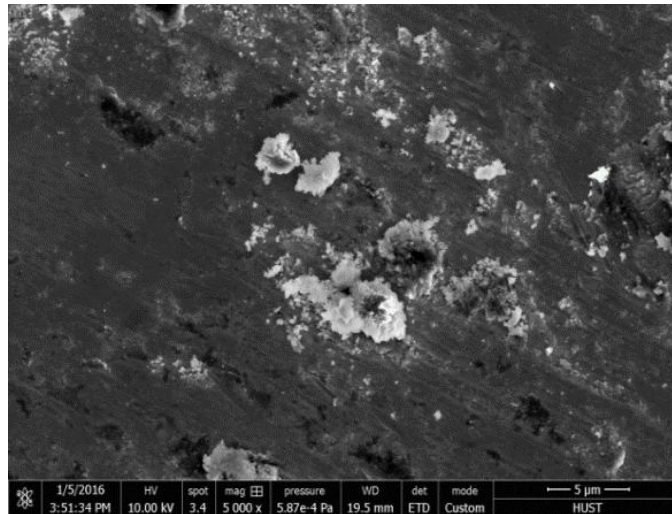
Figure 7: ESEM of Wear surface

5 Conclusion

1) H13 mould steel with self-medicated cored wire additive layer forming macro section without porosity, unfused and slag and other defects, and cold work mould steel Cr12MoV base material combination is good, the additive layer along the layer height direction microhardness, mechanical properties of high, weld state wear resistance is good;

2) Self-pharmaceutical cored wire for the ideal additive manufacturing wire and mould repair materials;

3) Arc fusion wire additive manufacturing technology provides an effective technical way for the green manufacturing and repair of metal parts.

Funding

REFERENCES

[1] YU Hongmei, LIU Haiqiong, ZHOU Hongmei, et al. Research on Applications of Remanufactory Technology for Die Steel Repair[J]. Electric Welding Machine, 2014, 44(11): 150-153.

[2] WANG Shijie, WANG Haidong, LUO Feng. Research Status of Metal Additive Manufacturing Technology Based on Arc[J]. MW Metal Forming, 2018(1): 19-22.

[3] XIONG Jun, XUE Yonggang, CHEN Hui, et al. Status and Development Prospects of Forming Control Technology in Arc-based Additive Manufacturing[J]. Electric Welding Machine, 2015, 45(9): 45-50.

[4] YANG Xiaoyu, LI Yan, ZHAO Pengkang, et al. Research Status and Challenges of Wire and Arc

Additive Manufacturing in Material Preparation[J]. Welding & Joining, 2018(8): 14-20.

[5] GENG Haibin, XIONG Jiangtao, HUANG Dan, et al. Research Status and Trends of Wire and Arc Additive Manufacturing Technology[J]. Welding & Joining, 2015(11): 17-21.

[6] XU Yunchao, CAO Renqiu, SHUI Li. Effect of Bi on Microstructure and Frictional Wear Properties of Al-20%Si Alloy[J]. Foundry, 2017, 66(6): 622-625.

[7] ZHAN Qiang, LIANG Yihui, DING Jialuo, et al. A Wire Deflection Detection Method Based on Image Processing in Wire + Arc Additive Manufacturing[J]. The International Journal of Advanced Manufacturing Technology, 2017, 89(1): 755-763.

[9] DENG Yu, YU Shengfu, QIU Hongbin, et al. Study on Microstructure and Properties for a New Kind of Arc Sprayed Martensitic Stainless Steel Wear Resistance Coatings[J]. Petro-Chemical Equipment, 2012, 41(4): 6-9.

[10] XIA Ranfei. Study on Forming Dimensions and Process Parameters Optimization of Wire Arc Additive Manufacturing[D]. Wuhan: Huazhong University of Science and Technology, 2016.

[11] HE Bo, CHU Shasha, ZHANG Hongyu, et al. Laser Forming Properties of Cobalt Base Superalloy[J]. Chinese Journal of Rare Metals, 2017, 41(4): 350-355.

[12] JI Ying ping, WU Su jun, XU Liu jie, et al. Effect of Carbon Contents on Dry Sliding Wear Behavior of High Vanadium High Speed Steel[J]. Wear, 2012, 294: 239-245.

Secondary Dynamic Coordinated Optimization of Tooth Profile for the Cycloid Gear in RV Reducers under Multi-factor Coupling

Zhenyu Wu*, Siyuan Liu, Tianxiang Zhang, Hang Deng, Zhiyu Dai

School of Physics and Mechatronic Engineering, Guizhou Minzu University, Guiyang 550025, China

*Corresponding author, E-mail: wzy5221027@163.com

Abstract:

The cycloid gear modification affects the meshing quality and transmission accuracy of RV speed reducers. However, there are few effective methods to find the optimal modification value. This paper adopts a secondary dynamic coordinated optimization method to obtain the optimal modification value. Firstly, by analyzing the meshing characteristics of the cycloid gear in RV speed reducers, the various factors which influence the RV speed reducers, transmission characteristics was established, and then the design variables were extracted. Secondly, on the constraints that transmission accuracy, contact stress, transmission smoothness and other transmission characteristics be satisfied, the maximum transmission torque was taken as the optimization objective and the meshing range of the cycloid gear was dynamically selected. Consequently, the maximum transmission torque and corresponding design variables can be obtained utilizing optimal algorithm. Finally, the meshing number and position of the cycloid gear can be adjusted, and the optimal solution satisfying all the constraints can be obtained after a second optimization. It is found that the cycloid gear profile modification obtained in this way can increase the rated load torque of RV reducers compared to existing products, and the transmission accuracy can also be enhanced. Consequently, a new solution can be provided for the profile modification of cycloid gears.

Keywords:

RV speed reducer, Cycloid gear, Modification, Optimization

1 INTRODUCTION

RV speed reducers, stemming from cycloid reducer, is a new kind of planetary gear transmission mechanism. Since 1986, it has become one of the main parts of industrial robots due to its large transmission ratio, high transmission efficiency and precision, small backlash, large stiffness, compact structure and so forth. Cycloid gear and pin gears are the main components that affect the transmission accuracy, backlash and stiffness in RV reducers. Ideally, the meshing points between cycloid gear and pin gears are half that of the pin gears. Whereas, owing to some machining and assembly errors as well as lubrication requirements, the tooth profile of cycloid gear will be modified to a certain value. Therefore, the meshing points will be less than half the pin gears. After reasonable modification, the torsional stiffness of the cycloid gear can be effectively increased to reduce the torsional deformation at rated load, and the transmission precision can be improved. Meanwhile, the modification can make the deformation at each meshing point more balanced and

reduce the contact stress to improve the load and anti-impact capability.

Extensive researches on the profile modification technology of cycloid gears have been conducted by many researchers. Reference [1] proposed that the optimal modified result should make the clearance between the new tooth profile and the original tooth profile generated by equidistant and shift modification as small as possible on the premise of maintaining specific radial clearance. So there are four kinds of combined modification methods. The meshing stiffness of cycloid gear are various with different combined modification methods. And the positive equidistant plus negative radial-moving modification method can obtain the maximum meshing stiffness when the combined modification produced the maximum initial clearance of the same size [2]. The tooth profile of the cycloid gear is a smooth curve which can be segmented into several curves by analyzing the pressure angle at each position of cycloid gear tooth profile. The most efficient range is taken as the working section tooth profile, and then the modification value can be obtained by further calculation [3]. Reference [4] realized the control of contact force and contact stress of cycloid gear by adjusting the meshing clearance of five key points in the gear meshing section of cycloid gear after modification. In order to reduce the computation of finite element method, the mathematical method is used to calculate the force of each meshing point after the cycloid gear was modified. Then the deformation and contact stress of the cycloid gear can be analyzed more quickly and accurately after applying the corresponding loads of the meshing points in the finite element model [5]. The cycloid reducers contain many components which could affect the transmission characteristic of the reducers. So the influence of eccentric distance and the radius of pin gear on the tooth profile of cycloid gear are analyzed in reference [6]. During the transmission process, the meshing stiffness and torsional stiffness are changing with the time, reference [7] analyzed the influence of tooth profile modification and eccentric error on the time-varying meshing stiffness of cycloid gear. And it proved that the variation characteristics of meshing stiffness and torsional stiffness with time after modification. Because of the limitation of the Hertz theory, reference [8] demonstrated the influence of profile modification on stress distribution of cycloid gear meshing point by applying non-Hertz theory. In the field of dynamics, reference [9-10] analyzed the meshing characteristics during the cycloid gear transmission process by using dynamic model, providing a new constraint for cycloid gear tooth profile's modification.

The existing methods tend to treat the influence of various factors on the meshing performance separately and ignore the relationship between them. During the process of determining the modification value, the initial modification value is usually determined in advance. Then, the initial value is iteratively calculated until the reducer meets a specific performance requirement. For instance, if only the stress homogenization is pursued to improve stress condition, the influence between meshing range and efficiency will not be considered sufficiently, so the efficiency may not reach the required standards. Therefore, the modification value determined by this kind of method does not take the coupling effect of multi-factors into account. Actually, the RV speed reducer products are to be qualified as long as the performance index including transmission accuracy, torsional stiffness, load torque and other performance indicators exist within the allowable range. If a certain performance is pursued excessively, some other performances will be too low and unnecessary waste will appear. Thus, an appropriate and general method should be applied to calculate the optimal modification value so the results after modification can realize the global optimum on the premise of satisfying all requirements of a RV reducer.

Taking the influence of multi-factor coupling effect on the RV reducers into consideration, this paper establishes a coupled mathematical model of the meshing performance, influence factors and modification value to analyze the interaction between them; thereafter, in order to improve the load capacity and anti-impact capability of the RV speed reducers, the maximum torque of the cycloid gear after profile modification is taken as the objective function. Because the transmission torque is a function of torsional stiffness and torsional deformation, the contact stress, transmission stability, initial clearance and rated torque should also be satisfied while meeting the torsional stiffness and torsional deformation requirements. Therefore, this paper

takes the coupling influence factors as the constraints. Then, the modification of cycloid gear with the maximum transmission torque is calculated by genetic algorithm when all the constraint conditions are satisfied. At last, it is determined whether to adjust the relevant constraints to carry out the second dynamic coordination optimization according to the condition of the meshing range after the first optimization. Thus, the optimum profile modification value can be obtained, which can make the meshing performance of a speed reducer reach the optimum.

2 CHARACTERISTIC PARAMETERS

2.1 Geometric parameters of cycloid gear

In the process of transmitting torque, there is an elastic deformation on the meshing points between cycloid gear and pin gears, which leads to a transmission error. The cycloid gear is regarded as an ideal rigid body, and the relative displacement caused by elastic deformation between the cycloid gear and pin gear is equivalent to the movement of the pin gear, as shown in Figure 1.
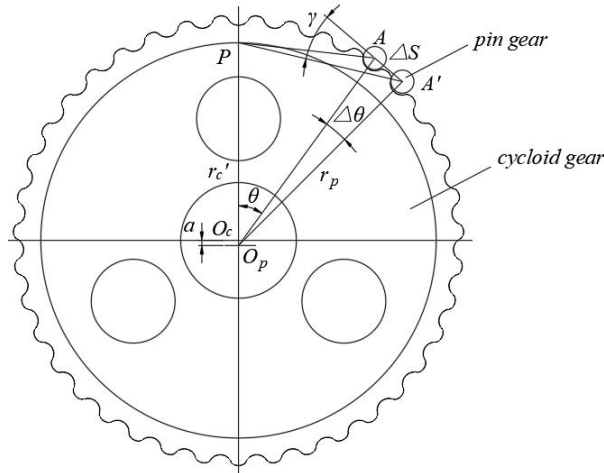
Figure 1: Transmission error diagram

where θ is the phase angle of the meshing point. a is the eccentric distance. r_c' is the distance from the pitch point P to the cycloid gear center O_c. r_p is the distance form pin center to O_p. $\Delta\theta$ is the angular deformation. A is the initial position of the pin center. A' is the position of the pin center after angular deformation. ΔS is the circumferential displacement of the pin center. ΔS_p is the equivalent displacement of the pin center along the normal direction PA', i.e. $\Delta S_p = \Delta S \cdot \cos\gamma$. The geometric relationship is as follows:

$$PA = \sqrt{(r_c' + a)^2 + r_p^2 - 2(r_c' + a)r_p \cos\theta}$$

$$PA' = \sqrt{(r_c' + a)^2 + r_p^2 - 2(r_c' + a)r_p \cos(\theta + \Delta\theta)}$$

$$\Delta S_p = r_p \cdot \frac{\pi}{180} \cdot \Delta\theta \left[\begin{array}{l} \sin\frac{\Delta\theta}{2} \cdot \frac{r_p - (r_c' + a)\cos(\theta + \Delta\theta)}{\sqrt{(r_c' + a)^2 + r_p^2 - 2(r_c' + a)r_p \cos(\theta + \Delta\theta)}} \\ + \cos\frac{\Delta\theta}{2} \cdot \frac{(r_c' + a)\sin(\theta + \Delta\theta)}{\sqrt{(r_c' + a)^2 + r_p^2 - 2(r_c' + a)r_p \cos(\theta + \Delta\theta)}} \end{array} \right] \tag{1}$$

$$L = \frac{r_c' r_p \sin(\theta + \Delta\theta)}{\sqrt{(r_c' + a)^2 + r_p^2 - 2(r_c' + a)r_p \cos(\theta + \Delta\theta)}} \tag{2}$$

After the profile modification of the cycloid gear, there will be initial clearances between the cycloid gear and the pin gear in the other positions when one of the cycloid gear tooth meshes with a certain pin gear [11-12].

The clearance $\Delta(\theta)_i$ along the normal direction of the initial clearance PA' can be calculated by Eq.(3).

$$\Delta(\theta)_i = \Delta r_{rp}\left(1 - \frac{\sin\theta_i}{\sqrt{1+K^2-2K\cos\theta_i}}\right) - \frac{\Delta r_p\left(1-K\cos\theta_i-\sqrt{1-K^2\sin\theta_i}\right)}{\sqrt{1+K^2-2K\cos\theta_i}}$$ (3)

Where K is the short width coefficient. Here, $K = \frac{az_p}{r_p}$.

2.2 Meshing stiffness of cycloid gear

During the meshing process of cycloid gear, the elastic deformation size can be approximately calculated by Hertz formula [13-14]. The extrusion deformation value of the pin gear can be calculated by Eq.(4).

$$t_z = \frac{4F_i\rho_c(1-\mu^2)}{\pi bEr_{rp}}$$ (4)

The extrusion deformation value of the cycloid gear tooth can be calculated by Eq.(5).

$$t_c = \frac{4F_i\rho_c(1-\mu^2)}{\pi bE\rho_i}$$ (5)

Where F_i is the force at the $i-th$ meshing point. E is the elastic modulus. μ is the Poisson ratio. b is the thickness of the cycloid gear. r_{rp} is the radius of the pin gear. ρ_i is the curvature radius of the cycloid gear tooth profile at the $i-th$ meshing point. ρ_c is the equivalent curvature radius at the $i-th$ meshing point. ρ_c can be calculated by Eq.(6-7).

$$\rho_c = \frac{\rho_i \cdot r_{rp}}{\rho_i - r_{rp}}$$ (6)

$$\rho_i = \frac{(r_p+\Delta r_p)(1+K'^2-2K'\cos\theta)^{\frac{3}{2}}}{K'(z_p+1)\cos\theta-(1+z_pK'^2)} + \left(r_{rp}+\Delta r_{rp}\right)$$ (7)

Because the elastic deformation of the meshing point is very small, so this paper considers the relationship between the elastic deformation and the contact force as a linear relation, which can meet the accuracy requirement [3]. The meshing stiffness of the pin gear can be calculated by Eq.(8).

$$k_z = \frac{F_i}{t_z} = \frac{\pi bEr_{rp}}{4\rho_c(1-\mu^2)}$$ (8)

The meshing stiffness of the cycloid gear can be calculated by Eq.(9).

$$k_c = \frac{F_i}{t_c} = \frac{\pi bE|\rho_i|}{4\rho_c(1-\mu^2)}$$ (9)

According to Eq.(6-7), it can be deduced that the meshing stiffness of a single pair of gear teeth is as follows.

$$k = \frac{k_z k_c}{k_z+k_c} = \frac{\pi bE|\rho_i|(\rho_i-r_{rp})}{4\rho_i(1-\mu^2)(r_{rp}+|\rho_i|)}$$ (10)

The relationship between the meshing stiffness of a single pair of teeth and the curvature radius of the cycloid gear tooth profile is shown in Figure 2.
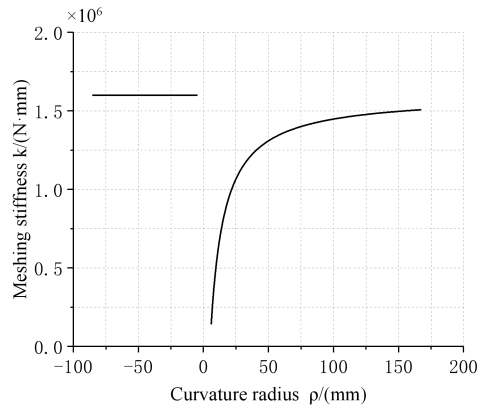

Figure 2: Variation of the meshing stiffness with curvature radius

When the cycloid gear profile is convex, the curvature radius is negative and the contact stiffness is a fixed value, which is independent of the curvature radius. When the tooth profile of cycloid gear is concave, the curvature radius is positive, and the contact stiffness is proportional to the curvature radius.

3 MULTI-FACTORS COUPLING MODEL

For a specific type of RV reducers, the transmission accuracy is determined by the torsional stiffness of cycloid gear when the load torque is constant during the transmission of torque. According to the equation of torsional stiffness [9]:

$$C = \sum C_j = \sum k_j \cdot L_j^2 \tag{11}$$

Where j is the meshing point. C_i is the torsional stiffness at the $i-th$ meshing point. k_j is the meshing stiffness at the $i-th$ meshing point. L_j is the arm of force at the $i-th$ meshing point. The quantity and position of the meshing points chang with the meshing range. And the corresponding meshing stiffness and arm of force will be quite different, which means the torsional stiffness generated at each meshing point is different. Therefore, the total torsional stiffness are determined by the meshing range.

The equation of the transmission accuracy is

$$\Delta\theta = \frac{T}{C} \tag{12}$$

The transmission accuracy is determined by torsional stiffness when the load torque is constant. As shown in Figure 3, there is a maximum torsional stiffness when the meshing range is within the peak and its adjacent interval of the torsional stiffness at a single meshing point.
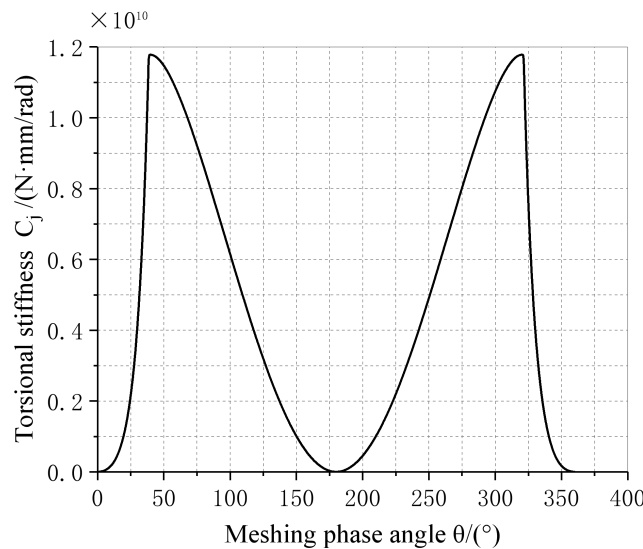
Figure 3: Variation of the torsional stiffness at a single meshing point

According to the Eq.(1), the torsional deformation is a function of equivalent deformation of the pin gear at the meshing point and the position of the meshing point. The relationship between them is shown in Figure 4.

After the profile modification of the cycloid gear, there will be initial clearance between the cycloid gear and the pin gears during the transmission. When the equivalent deformation is greater than the initial clearance, the cycloid gear is meshed with the pin gear, which results in contact deformation. Otherwise, the meshing does not occur. As shown in Figure 5, the intersection area between the equivalent deformation curve and the initial clearance curve is the meshing range in which contact deformation occurs. And the difference of the vertical coordinate values is the contact deformation at each meshing point.
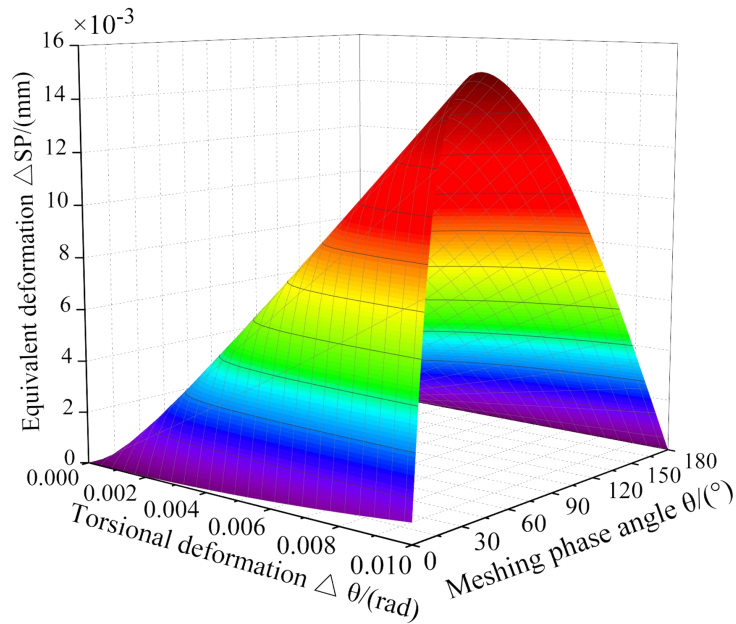
Figure 4: Variation of the torsional deformation with the equivalent deformation and the phase angle of meshing
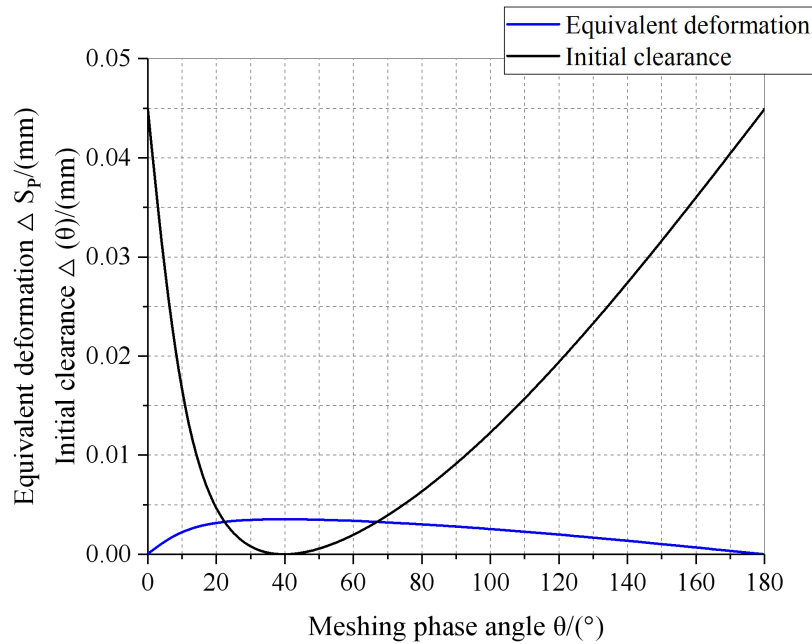
Figure 5: Variation of the equivalent deformation and initial clearance with phase angle of meshing

The contact stress between the cycloid gear and pin gear can be calculated by Eq.(13).

$$\sigma_H = 0.418\sqrt{\frac{EF_i}{b\rho_c}} = 0.418\sqrt{\frac{Ek_i(\Delta S_{pi} - \Delta(\theta)_i)}{b\rho_c}} \tag{13}$$

The contact stress of cycloid gear is determined by contact deformation, meshing stiffness and composite curvature radius of meshing point. The smaller the contact stress value is, the greater the contact force that can be borne by the meshing point, which means the greater the torque can be transmitted. However, the transmission accuracy will also change with the transmitted torque. As shown in Figure 6, the overall performance of cycloid gear can be adjusted by changing the profile modification value of the cycloid gear.
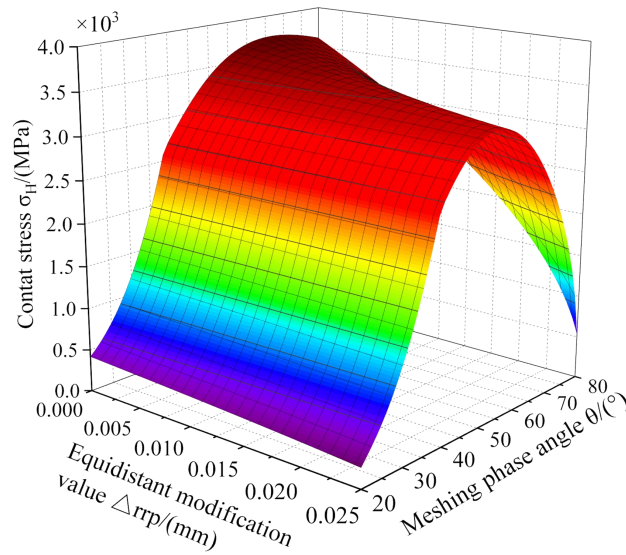
(a) Variation of contact stress with equidistant modification
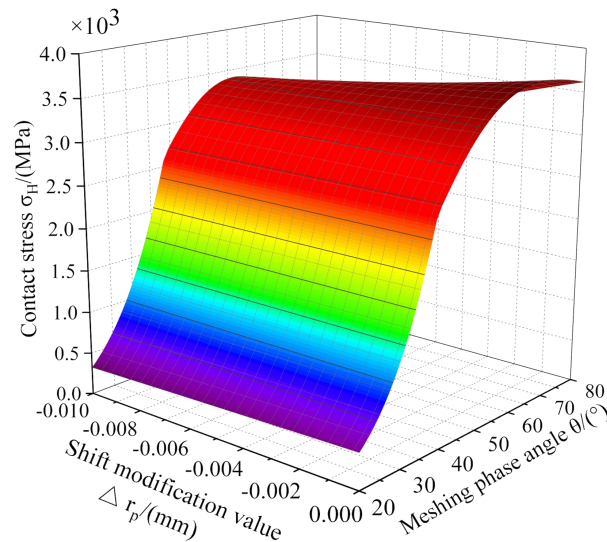
(b) Variation of contact stress with shift modification

Figure 6: Variation of contact stress with profile modification

In summary, the change of profile modification of the cycloid gear will lead to the change of initial clearance and curvature radius. The meshing range is determined by the values of the initial clearance and equivalent deformation. The meshing stiffness is determined by the meshing range and the curvature radius at the meshing point. Thus, the torsional stiffness of cycloid gear can be determined. And the transmission accuracy under different load torque is finally controlled. Meanwhile, the equivalent deformation of cycloid gear is determined by the transmission accuracy and the meshing points. And the equivalent deformation, initial clearance and curvature radius of each meshing point determine the contact stress at each meshing point. The smaller the contact stress, the more torque the cycloid gear can transmit, which causes the change of the transmission accuracy. The coupling relationship between the performances of cycloid gear is shown in Figure 7.
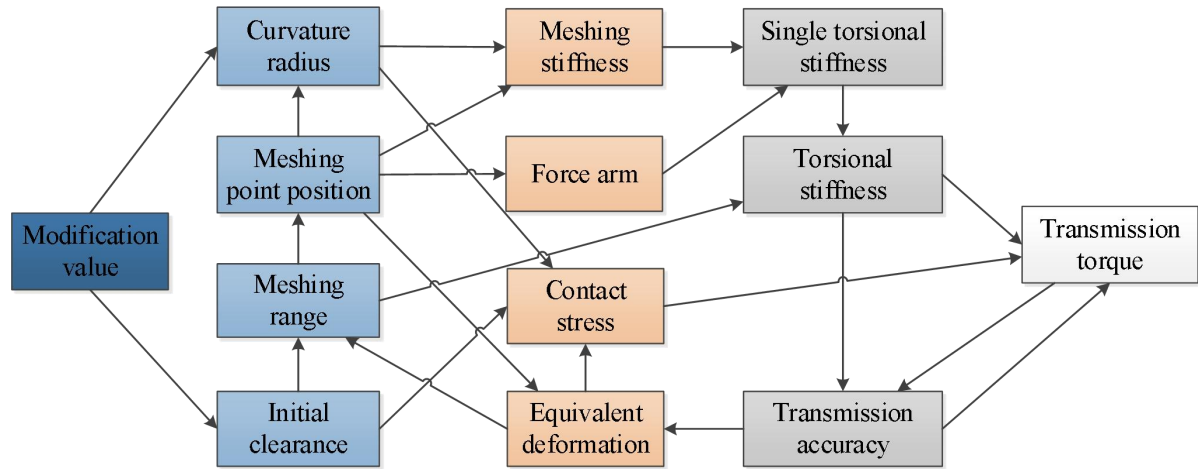
Figure 7: Coupling relationship between the performances of cycloid gear

4 DYNAMIC OPTIMAL DESIGN FOR THE CYCLOID GEAR

In this paper, the tooth profile modification of the existing RV reducers is optimized and its structure size is not changed. The tooth profile modification of cycloid gear is usually divided into three method: equidistant modification, radial-moving modification and rotated angle modification, which represented by Δr_{rp}, Δr_p and $\Delta\delta$ respectively.

4.1 Design variables

Because the rotated angle modification is more complicated, it will greatly increase the grinding time, so the combination of equidistant modification and radial-moving modification is often adopted [1]. As shown in Figure 7, the value of transmission torque is determined by torsional stiffness and transmission accuracy $\Delta\theta$. And torsional stiffness is a function of the modification. Therefore, the design variables of the whole optimization are $\Delta\theta$, Δr_{rp} and Δr_p.

4.2 Objective function

In the performance parameters of RV reducers, transmission accuracy, stiffness, reliability, lubrication and other performances are the requirements that must be satisfied. At the same time, greater transmission torque means higher load capacity and anti-impact capability. So the objective function is

$$T\left(\Delta\theta, \Delta r_{rp}, \Delta r_p\right)_{max} \tag{14}$$

4.3 Constraint conditions

As mentioned above, the transmission accuracy, contact stress, lubrication requirements, minimum curvature radius and rated load should be satisfied when optimizing the profile modification of cycloid gear. So the constraint conditions are as follows.

4.3.1 Transmission accuracy constraint

In this paper, the transmission accuracy is the angle deviation caused by the elastic deformation between the cycloid gear and the pin gear. The maximum value of the transmission accuracy can be selected according to

its influence on the sensitivity of total transmission accuracy [15-16]. Therefore, the constraint condition is

$$0 < \Delta\theta < \eta\varphi \tag{15}$$

Where η is the proportional coefficient of influence on sensitivity. φ is the transmission accuracy.

4.3.2 Contact stress constraint

The contact stress at meshing points of cycloid gear should not exceed allowable contact stress σ_{HP}. Because the cycloid gear and the pin gear are usually of the same material, the constraint condition of the contact stress is

$$\sigma\sqrt{\frac{EF_i}{b\rho_c}}_{HP_{Hmax}} \tag{16}$$

4.3.3 Modification constraint

The minimum clearance between the root of the cycloid gear and the pin gear should be greater than the clearance $\Delta_{\min}$ which is used to generate oil film for lubrication. Therefore, the constraint condition is

$$\Delta r_{rp} + \Delta r_p \geq \Delta_{min} \tag{17}$$

Meanwhile, there are clearances between the cycloid gear and the pin gear in the other positions when one of the cycloid gear tooth meshing with a certain pin gear. As shown in Figure 5, because the initial clearance is a concave function, the second derivative is greater than 0. And when $\theta = \arccos K$, $\Delta(\varphi) = 0$. Therefore, the constraint condition is

$$\frac{d^2\Delta(\theta)_i}{d\theta_i} = \Delta r_{rp} - \Delta r_p \frac{1}{\sqrt{1-K^2}} > 0 \tag{18}$$

4.3.4 Minimum curvature radius constraint

During the transmission, the top cut and sharp corner must be avoided for the stationarity of the transmission. If the curvature radius of cycloid gear tooth profile is too small, it will lead to the top cut and sharp corner. As shown in Figure 8, the concavity and curvature radius of cycloid gear tooth profile will change with the meshing phase angle. In order to avoid the top cut or sharp corner, the curvature radius of cycloid gear tooth profile must satisfy the minimum curvature radius requirement [12]. Therefore, the constraint condition is

$$\rho_{i\,convave} \geq \frac{(1-K)^2}{z_pK-1}r_p \tag{19}$$

$$|\rho_i|_{convex} \geq \begin{cases} r_p\sqrt{\frac{27(1-K^2)(z_p-1)}{(z_p+1)^3}}, & 1 > K > \frac{z_p-2}{2z_p-1} \\ \frac{(1+K)^2}{z_pK+1}r_p, & \frac{z_p-2}{2z_p-1} \geq K \end{cases} \tag{20}$$
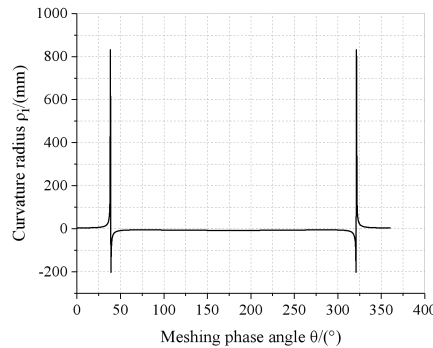
Figure 8: Variation of curvature radius with meshing phase angle

4.3.5 Transmission torque constraint

According to reference [13], because the distribution of the force is not uniform during the transmission, the torque transferred by a single cycloid gear is

$$T_c = 0.55T \tag{21}$$

Where T is the rated load of the RV reducers. As shown in Figure 9, the torque applied to the center of the cycloid gear is generated by the force at the meshing points, which form the transmission torque.
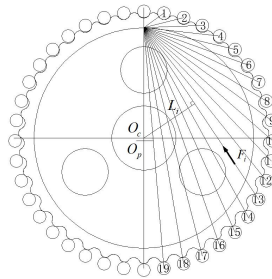
Figure 9: Torque distribution

The sum of the torque generated at the meshing points should be not less than the rated load torque, so the constraint condition is

$$T_c = \sum \left(k_i \cdot \left(\Delta S_{pi} - \Delta(\theta)_i \right) L_i \right) \geq 0.55T \tag{22}$$

Where k_i is the meshing stiffness of a single pair of teeth at the $i - \text{th}$ meshing point.

4.4 Optimization program

According to the meshing characteristic of cycloid gear, different modification value will cause different meshing range. If the meshing rang is selected only according to the design experience, the calculation amount is too large and it is difficult to get the optimal solution. Therefore, the key of the optimum design is to realize the automatic selection and calculation of the meshing range by appropriate method. And the optimal value under the constraint conditions is obtained by calculation. This paper selected the meshing points automatically by computer programs. And then the genetic algorithm is used to optimize the calculation[17]. The calculation process is shown in Figure 10.
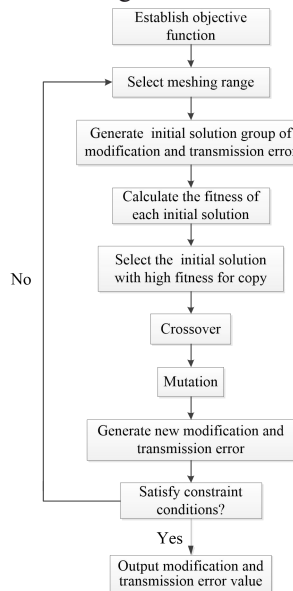
Figure 10: Flow diagram of optimization calculation

4.5 Secondary optimization

During the transmission, the force arm is very short when the meshing phase angle θ is too small, which will lead to the decrease of transmission efficiency. Meanwhile, when the meshing phase angle is too large, the relative sliding speed between the cycloid gear and pin gear will be too large, which leads to the increase of power loss and the decrease of efficiency. In addition, when the phase angle is too large, the curvature radius of cycloid gear is smaller, and the contact stress will increase, resulting in scuffing. The recommended range of meshing phase angle is $25° < \theta < 100°$ [12]. Therefore, while optimizing the modification of cycloid gear, the meshing range of cycloid gear must be controlled.

According to reference [3], the adjustment of meshing range can be realized by changing the symbol of equidistant modification and radial-moving modification. Therefore, when the first optimization calculation is finished, the quantity and position of meshing points can be adjusted by increasing or decreasing the meshing range according to the distribution of the meshing range. As shown in Figure 11, the combination of positive equidistant and negative radial-moving modification can increase the meshing range compared with that of positive equidistant and positive radial-moving modification. Therefore, the meshing range can be changed through setting the value interval of equidistant and radial-moving modification. And the more suitable meshing range can be obtained.
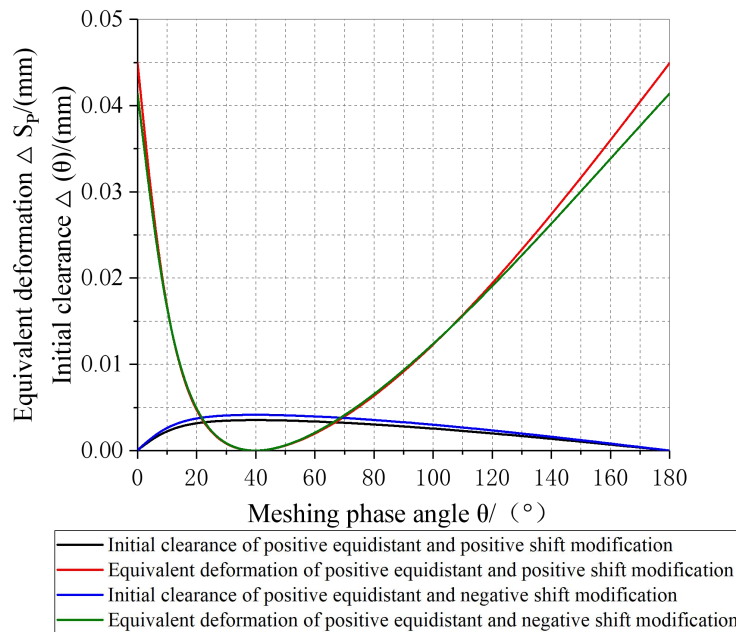
Figure 11: Variation of the meshing range with modification vale

5 VERIFICATION OF OPTIMIZATION RESULT

In this paper, genetic algorithm is used to optimize profile modification of the cycloid gear in RV-40E reducers. As shown in Figure 12, because the interval of the solution satisfying the constraint condition is very small, the optimization calculation can become stable at a rapid pace. When the genetic algorithm calculation results evolve to the 13th generation, the optimal solution is obtained. Therefore, the maximum torque that can be transmitted by a single cycloid gear is 275.3N·m. The transmission accuracy $\Delta\theta$ is 0.01rad, the equidistant modification value Δr_{rp} is 0.019mm and the radial-moving modification value Δr_p is -0.01mm.

The cycloid gear of RV-40E reducers parameters are shown in Table 1.

Table 1 Cycloid gear of RV-40E reducers parameters

Parameter	Value
Cycloid gear tooth number	39
Pin gears number	40
Eccentric distance (mm)	1.25
Cycloid gear thickness (mm)	9
Pin gear diameter (mm)	3
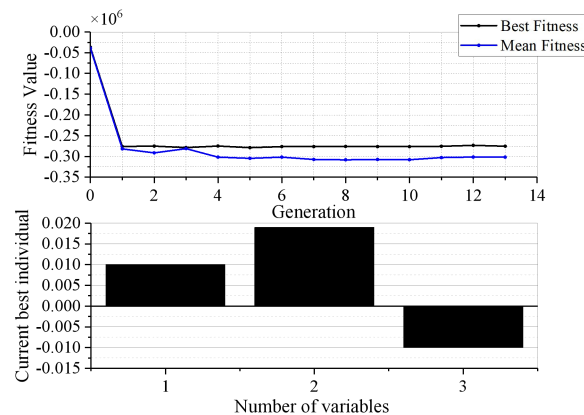
Figure 12: Optimization calculation result

5.1 Verification of multi-factors coupling optimization result by finite element analysis

According to the modification of cycloid gear after optimization, the model of cycloid gear is established by FEM. Because the cycloid gear is bolted between the planet carrier and rigid disk, so the cycloid gear can be regarded as a rigid body. Therefore, there is only a central hole on cycloid gear to apply equivalent torque for convenience of calculation. Then, the cycloid gear model is meshed with hexahedron elements. The contact element is established between the 1th to 19th pin gears and the corresponding cycloid gear tooth. The result of finite element analysis is shown in Figure 13.
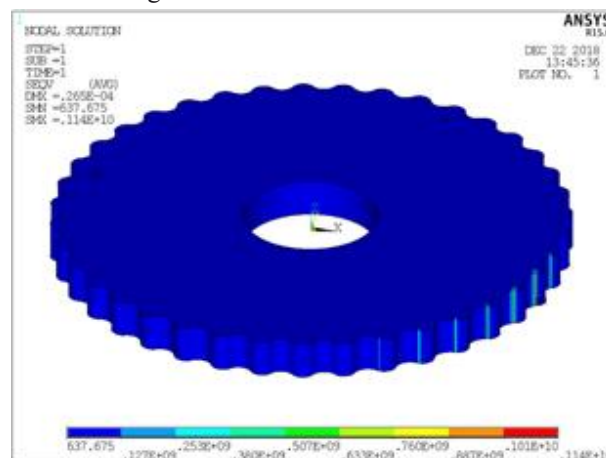
Figure 13: Finite element analysis result

The meshing points between cycloid gear and pin gear are 3th to 9th, which meets the requirements of

meshing range 25°-100°. The maximum contact deformation is 0.0265mm and the maximum stress is 1140MPa, which meets the design requirements.

5.2 Verification of single factor optimization result by finite element analysis

If only the stress homogenization is considered as the optimization objective, and multi-factors coupling is not considered, the finite element analysis result is shown in Figure 14.
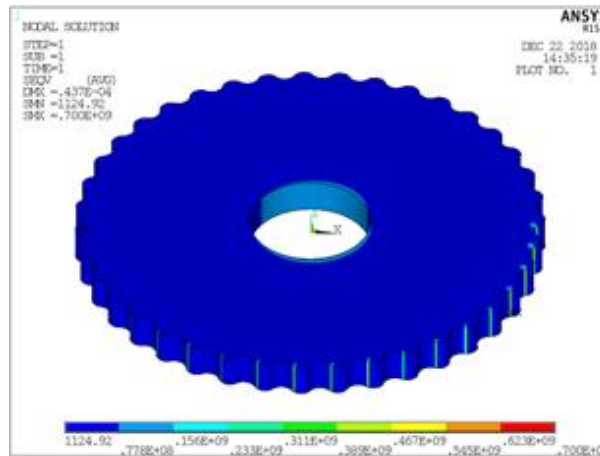
Figure 14: Finite element analysis result

The deformation of cycloid gear is 0.0437mm which is more than 0.0265mm after considering multi-factors coupling optimization, i.e. the transmission accuracy is lower. And the maximum contact stress is 700MPa which is less than 1140MPa after considering the multi-factors coupling optimization. But, according to the requirement of cycloid gear meshing range, the meshing points is form 2th to 16th, which is obviously not satisfied the requirement of meshing range 25°-100°.

In conclusion, considering the multi-factors coupling and the optimum modification determined by the optimization method with transmission torque as the optimization objective can meet the requirements of multiple performance indexes of cycloid gear simultaneously.

5.3 Experiment verification

In this experiment, the cycloid gears with the modification value obtained by multi-factors coupling optimization are machined, and the RV reducers with this cycloid gears are assembled. Then the torsional stiffness, transmission accuracy and transmission efficiency are compared between this RV reducers and that produced by a company. This test is carried out on the comprehensive performance test-bed of RV reducers. As shown in Figure 15, the test-bed can be used to detect the efficiency, torsional stiffness, backlash, transmission error and startup torque of the RV reducer within 5000N.m. Meanwhile, the temperature, vibration and noise of the reducer can be detected in real time. The double-range torque sensor (200N.m/20N.m) is adopted on the input terminal. The double-range torque sensor (5000N.m/500N.m) is adopted on the output terminal. And the drive motor is controlled by Siemens servo motor. The measurement accuracy of torque is ±0.1%FS, the measurement accuracy of rotational speed is ±1r/min. The fastest update speed of angle measurement is 1ms, and the speed of data recording is 100ms each time. The input terminal adopts the rotary encoder with the measurement accuracy of ±1.5″ , and the output terminal adopts the rotary encoder with the measurement accuracy of ±2.38″ , which ensures the measurement accuracy of the angle error.
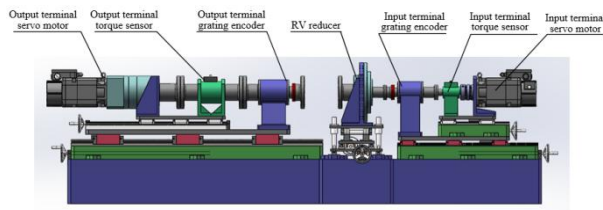
Figure 15: Comprehensive performance test-bed of RV reducers

5.3.1 Torsional stiffness experiment

This experiment is used to detect the torsional stiffness of cycloid gear transmission, that is, the torsional stiffness of output terminal. So the input terminal is fixed by the fixture of the test-bed in order to eliminate the influence of planetary gear part on the experiment result. During the detection, the servo motor and reducer on the output terminal of the test-bed applied torque to the RV reducers, and the torque was gradually increased from 0 N·m to the rated torque. And then the torque was applied in the opposite direction, which gradually loaded from 0 N·m to the rated torque. During the experiment, the driving torque and angle variation are monitored in real time by the torque sensor and rotary encoder of the output terminal. And the data is recorded every 0.1s. The experiment results are shown in Figure 16.
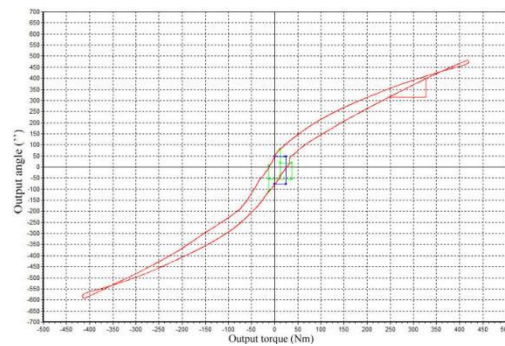
(a) Torsional stiffness experiment result of a RV-40E reducer produced by a company
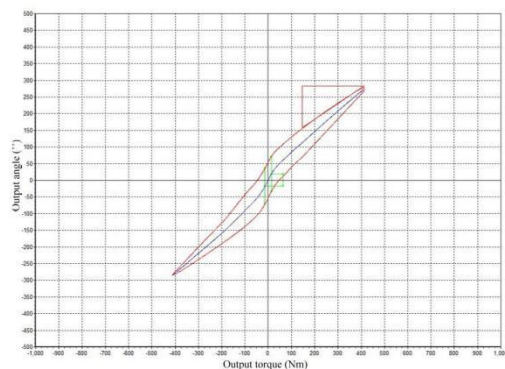
(b) Torsional stiffness experiment result of a RV-40E reducer after optimization
Figure 16: Torsional stiffness experiment results of a RV-40E reducer

The experiment results can be directly obtained from the software interface. Because the stiffness experiment is to apply torque in clockwise and counterclockwise directions, the backlash of the RV reducers is also measured at the same time. It is shown that the torsional stiffness of the optimized RV reducers is significantly increased and the backlash is reduced, which proves that this optimization method in improving torsional stiffness and reducing the backlash of the RV reducers is feasible.

5.3.2 Transmission accuracy experiment

When measuring the transmission accuracy, the output terminal applied a constant load of 50N·m, and the input terminal applied torque and rotational speed. The rotary encoder was used to monitor the rotation angle of the input terminal and output terminal in real time. And the data is recorded every 0.1s. Then the rotation angle of the input terminal is divided by the transmission ratio, and the difference between this result and the rotation angle of the output terminal is the real-time transmission accuracy. The experiment results are shown in Figure 17.

(a) Transmission accuracy experiment result of a RV-40E reducer produced by a company
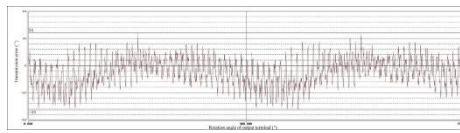
(b) Transmission accuracy experiment result of a RV-40E reducer after optimization
Figure 17: Transmission accuracy experiment results of a RV-40E reducer

The results indicate that the total transmission accuracy presents a periodic change, which is mainly caused by the periodic change of the meshing stiffness during the transmission of the RV reducers. And the variation of local transmission accuracy is mainly caused by the vibration of reducer and the change of meshing clearance. Under the load of 50N·m, the transmission accuracy of the optimized RV reducers is significantly improved, which is in the interval of −33'' to 24'' . Therefore, the transmission accuracy of the optimized RV reducer can satisfy the accuracy requirement.

5.3.3 Transmission efficiency experiment

During the detection of transmission efficiency, torque and constant speed are applied at the input and output terminals respectively. When the torque is gradually increasing to the rated torque, the data of input and output torque and speed are collected in real time. The data is recorded every 0.1s, and the real-time transmission efficiency can be obtained by calculation. The experiment results are shown in Figure 18.

(a) Transmission efficiency experiment result of a RV-40E reducer produced by a company

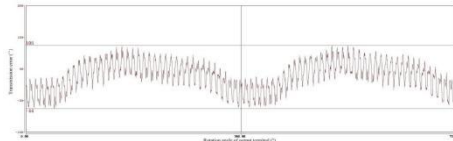*(b) Transmission efficiency experiment result of a RV-40E reducer after optimization*
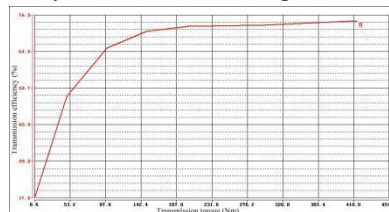*Figure 18: Transmission efficiency experiment results of a RV-40E reducer*
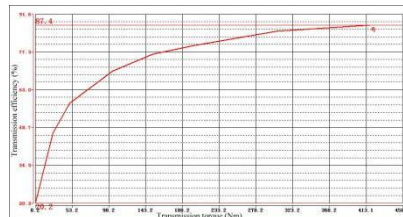
It is concluded that the transmission efficiency is proportional to the load torque, and the transmission efficiency is highest when the load torque is maximum. The transmission efficiency of the optimized RV reducers has been improved, strongly proving the feasibility of the optimization method in improving the transmission efficiency in the RV reducers.

6 CONCLUSIONS

(1)Since the influence of the cycloid gear modification value on the meshing performance for RV reducers suffers from coupling effect of multi-factors, the coupling mathematical model among meshing performance, influence factors and modification value is established, which provides theoretical support for the establishment of mathematical model for optimization.

(2)The genetic algorithm is used to optimize the mathematical model of cycloid gear in each meshing range. Then, the optimum modification value and maximum transmission torque of cycloid gear are obtained after the first optimization.

(3)A secondary dynamic optimization method is proposed in this paper. On the basis of the first optimization result and the corresponding meshing condition of the cycloid gear, this method properly adjusts the value range of cycloid gear modification properly. Then a more suitable meshing range and the corresponding optimum modification value are obtained.

(4)According to the experiment results, the proposed secondary dynamic optimization method considering multi-factors coupling effects in this paper can obtain the optimal profile modification value for the cycloid gear. The requirements for multiple meshing performance can be satisfied at the same time using this method.

Funding

REFERENCES

[1]Chen, Z. Y.: Error modeling and tooth profile modification of cycloid on RV reducer, Tianjin: Tianjin University, 2013.

[2]Guan, T. M.: The optimum profile modification on cycloid disks in the cycloid gearing mechanism with small teeth difference, China Mechanical Engineering, 13, 811-814, 2002.

[3]Li S. T.: Design and strength analysis methods of the trochoidal gear reducers, Mechanism and Machine Theory, 81, 140-154, 2014.

[4]Li, X., Chen, B. K., Wang, Y. W. and Chin, L. T.: Mesh stiffness calculation of cycloid-pin gear pair with tooth profile modification and eccentricity error, Journal of Central South University, 25, 1717-1731, 2018.

[5]Liu, J. Y., Mastumura, S., Chen, B. K. and Houjoh, H.: Torsional stiffness calculation of double-enveloping cycloid drive, Journal of Advanced Mechanical Design, Systems, and Manufacturing, 6, 2-14, 2012.

[6]Meng, Y. H., Wu, C. L. and Ling, L. P.: Mathematical modeling of the transmission performance of 2K–H pin cycloid planetary mechanism, Mechanism and Machine Theory, 42, 776-790, 2007.

[7]Ren, Z. Y., Mao, S. M., Guo, W. C. and Zheng, G.: Tooth modification and dynamic performance of the cycloid drive, Mechanical System and Signal Processing, 85, 857-866, 2017.

[8]Tsai, S. J., Chang, L. C. and Huang, C. H.: Design of cycloid planetary gear drives with tooth number difference of two, Forschung im Ingenieurwesen, 81, 325-336, 2017.

[9]Wang, J. N.: Study on the relationship between the stiffness of RV reducer and the profile

modification method of cycloid-pin wheel, Intelligent Robotics and Applications, 721-735, 2016.

[10]Yu, H. L., Yi, J. H., Hu, X. and Shi, P.: Study on teeth profile modification of cycloid reducer based on non-Hertz elastic contact analysis, Mechanics Research Communications, 48, 87-92, 2013.

[11]Wang, J., Luo, S. M. and Su, D. Y.: Multi-objective optimal design of cycloid speed reducer based on genetic algorithm, Mechanism and Machine Theory, 102, 135-148, 2016.

[12]Xu, L.X. and Yang, Y. H.: Dynamic modeling and contact analysis of a cycloid-pin gear mechanism with a turning arm cylindrical roller bearing, Mechanism and Machine Theory, 104: 327-349, 2016.

[13]Zhang, Z.: Manual for practical gear calculation, China Machine PRESS, China, 2010.

[14]Zhu, X. L.: Manual of gear drive design, Chemical Industry Press, China, 2005.

[15]Zhang, D. W., Wang, G. and Huang, T.: Dynamic formulation of RV reducer and analysis of structural parameters, Chinese Journal of Mechanical Engineering, 37, 69-74, 2001.

[16]Zhu, Z. X., Dong, H. J. and Han, L. S.: Sensitivity analysis of error combination to transmission precision of RV reducer, Mechanical Design, 25, 69-72, 2008.

Research on Multimodal Large-Model-Driven Mining Safety Early Warning Mechanism

Changwen Wu*

Wuhan Yishikong Technology Co., Ltd., Wuhan, Hubei 430000, China

***Corresponding author, E-mail: woochangwen@163.com**

Abstract:

Mining safety production is a high-risk sector within the industrial system, facing severe challenges such as complex geological conditions, dynamic environmental changes, and intertwined human operation risks. Traditional single-modal monitoring technologies exhibit significant limitations in real-time perception and intelligent decision-making, failing to meet the demands of modern mining safety management. To address these issues, this paper proposes a multimodal large-model-driven mining safety early warning mechanism. By leveraging multimodal data integration and cross-modal learning, the mechanism achieves comprehensive perception and accurate early warnings for mining operations. The research encompasses multimodal data collection and processing, large-model design and implementation, as well as the construction and application of the safety warning mechanism. This approach significantly enhances the intelligence level of mining safety management and accident prevention, providing essential technical support for the development of smart mining.

Keywords:

Mining Safety; Multimodal Technology; Large Model; Safety Early Warning; Smart Mining

1 INTRODUCTION

Mine safety has consistently been a critical area of focus within industrial production. As mining operations expand in scale and working environments grow increasingly complex, frequent mining accidents pose a severe threat to the lives of personnel and production efficiency. Traditional mine safety early warning technologies primarily rely on single data sources and rule-driven systems. For instance, environmental parameters such as methane concentration, temperature, and humidity are monitored via sensors, with alarms triggered by predefined thresholds. Alternatively, statistical analysis methods based on historical data are employed to predict potential hazardous situations. However, these approaches exhibit significant limitations. They suffer from narrow data sources that fail to comprehensively reflect the complex mining environment, lack flexibility in rule-based systems to address sudden and diverse safety risks, and insufficient capability in traditional models to handle non-linear data relationships and multimodal information. Consequently, the accuracy and timeliness of early warnings remain suboptimal. In recent years, the rapid advancement of artificial intelligence has seen machine learning and deep learning technologies progressively integrated into mine safety early warning systems. For instance, time series analysis techniques are employed to predict equipment failures, while image recognition technologies monitor operational environments within mining areas. Nevertheless, these approaches remain predominantly reliant on unimodal data, struggling to fully leverage the multimodal data resources inherent in mining operations and thus failing to comprehensively reflect the intricate characteristics of complex working environments. Consequently, harnessing multimodal

technologies to enhance the efficacy of mine safety early warning systems has emerged as a critical research focus.

2 CURRENT SITUATION ANALYSIS

In recent years, large language models have emerged as a significant breakthrough in artificial intelligence, demonstrating formidable potential particularly in natural language processing and computer vision applications. Models such as GPT (Generative Pre-trained Transformer) for natural language processing and visual Transformers for computer vision possess robust feature extraction capabilities, cross-modal learning abilities, as well as versatility and transferability. Through training on vast datasets, these models can extract deep-level features from multimodal data and adapt to specific domain tasks with minimal fine-tuning. Within industrial safety, large models are primarily applied in fault detection, risk assessment, and intelligent monitoring. However, in the field of mining safety, their application remains in the early exploratory stages, with no mature solutions yet established. Multimodal technology achieves more comprehensive and precise analysis by integrating information from diverse data sources or modalities (such as text, images, audio, and video). Its core lies in data fusion and complementarity, where different modalities provide multidimensional insights into the same event, thereby overcoming the limitations of single-modality data. Multimodal technology has demonstrated significant application potential across numerous domains. Within mine safety, the introduction of multimodal technology can effectively integrate environmental monitoring data (such as gas concentration, temperature, humidity), video surveillance footage, textual records (like operational logs), and other data sources, thereby providing more comprehensive support for safety alerts. Despite achievements in industrial safety, applying multimodal technology and large models to mine safety presents several challenges. Firstly, multimodal data in mining environments exhibits heterogeneity and spatio-temporal inconsistency, making effective fusion a critical issue. Secondly, mine safety alerts demand real-time responsiveness, whereas current large models' computational complexity may compromise system timeliness. Furthermore, existing large models are predominantly general-purpose systems, necessitating further research into tailored designs addressing the specific requirements of mine safety. Consequently, developing a mine safety early warning mechanism based on multimodal large models—by integrating multimodal data and leveraging the cross-modal learning capabilities of large models—will enhance the accuracy and real-time responsiveness of mine safety alerts, thereby providing more reliable safety assurance for mining operations.

3 KEY TECHNOLOGY DESIGN AND IMPLEMENTATION

This study proposes a mine safety early warning mechanism based on multimodal large language models. By integrating multimodal data fusion with the cross-modal learning capabilities of large models, it achieves comprehensive perception and efficient early warning of mine operational environments. The mechanism's design encompasses multimodal data acquisition and processing, large model design and implementation, and the construction of a model-based safety early warning system.

3.1 Multimodal Data Acquisition and Fusion

The mining environment is complex and dynamic, with data originating from diverse sources including environmental monitoring, video surveillance, and textual records. These data exhibit modal diversity and spatio-temporal heterogeneity, making their effective collection and processing fundamental to designing early warning mechanisms.

Firstly, during the data collection phase, environmental monitoring data is primarily obtained through sensor networks deployed across the mining area, capturing parameters such as methane concentration, temperature,

humidity, and wind speed. Video surveillance data is gathered in real-time via cameras positioned throughout the mine, documenting worker behaviour and equipment operational status. Textual data originates from mining operation logs, equipment maintenance records, and historical accident reports. This multimodal data reflects the safety conditions of mining operations from multiple dimensions.

Secondly, during the data processing stage, a unified preprocessing workflow addresses the heterogeneity of multimodal data. This includes operations such as data cleansing, format conversion, and temporal alignment. During data cleansing, outliers and noise in sensor data are removed, while invalid frames in video data are discarded. Format conversion standardises disparate data formats into a unified input format. Temporal alignment synchronises multimodal data via timestamps, ensuring spatio-temporal consistency. Furthermore, to enhance data usability and information content, feature engineering techniques are employed for feature extraction and fusion across multimodal data.

The multimodal data fusion mechanism constructs a multi-level collaborative modelling framework by integrating heterogeneous modal information such as images, text, and audio. Its core lies in cross-modal feature alignment and dynamic semantic complementarity. This mechanism is typically organised across three levels: data-level and feature-level. Data-level fusion directly processes raw data, such as aligning LiDAR point clouds with camera images through calibration techniques to resolve spatio-temporal heterogeneity; Feature-level fusion employs deep learning models to extract high-dimensional abstract features from each modality, utilising attention mechanisms or graph neural networks to enable cross-modal interaction. Spatial features from video data are extracted via convolutional neural networks, semantic information from textual data is derived through natural language processing techniques, and these are combined with the temporal characteristics of sensor data to form multimodal feature vectors, thereby achieving multimodal data fusion.

3.2 Design and Implementation of Large Models

The large model design is grounded in the core principles of multimodal fusion and cross-modal learning, employing the Transformer architecture as its foundational framework. The Transformer has gained widespread application in natural language processing and computer vision due to its formidable capabilities in feature extraction and cross-modal learning.

In the model architecture design, a multimodal feature encoder was first constructed to address the characteristics of multimodal data. This encoder processes environmental monitoring data, video data, and text data independently, extracting high-level features from each modality.

During the feature fusion stage, a Cross-Modal Attention Mechanism is employed to integrate multimodal features. This mechanism enables complementary information exchange between modalities, yielding more expressive joint feature representations. Furthermore, to enhance the model's generalisation capability and robustness, a self-supervised learning strategy is adopted for model pre-training, leveraging unlabelled data to uncover latent intra- and inter-modal associations.

During model training and optimisation, a multi-task learning framework divides the mine safety early warning task into three sub-tasks: hazard factor identification, risk prediction, and early warning information generation. Shared model parameters enable joint optimisation across these sub-tasks. Concurrently, to address data distribution imbalances in mining environments, data augmentation techniques and weighted loss function strategies are employed to enhance the model's recognition capability for minority class samples.

3.3 Implementation of the Safety Early Warning Mechanism

Leveraging the multimodal learning capabilities of large language models, a mine safety early warning mechanism has been established to enable real-time hazard identification, risk prediction, and the generation of alert notifications.

During the hazard identification phase, the model analyses features across multimodal data streams to detect potential risk factors that could precipitate safety incidents. For instance, video data is scrutinised to identify instances of non-compliant operator behaviour, sensor readings are examined to detect environmental parameters exceeding safety thresholds, and textual data is mined to uncover latent risk points within historical records.

During the risk prediction phase, the model combines historical and real-time data, employing time series analysis and deep learning techniques to forecast risk trends within the mining environment. Examples include predicting methane concentration trajectories to assess explosion risks, and analysing equipment operational states to anticipate potential failures.

During the early warning generation phase, the model produces specific alerts based on identification and prediction outcomes, presenting these via a visualised interface to mine management personnel. For instance, upon detecting an abnormal rise in methane concentration, the system generates an alert stating: 'Methane concentration exceeds permissible limits; personnel should evacuate immediately.' When identifying non-compliant operations by personnel, the system issues a prompt: 'Worker not wearing safety helmet; rectify immediately.'

4 APPLICATION SCENARIO ANALYSIS

The multi-modal large-model-based mine safety early warning mechanism demonstrates significant practical value across multiple operational scenarios within mining environments. By deeply integrating multi-modal information such as sensor data, video surveillance footage, and textual records, this mechanism enables efficient risk perception and early warning within complex, dynamic mining conditions. Below, we conduct a detailed analysis of this early warning mechanism's application within typical mining scenarios, demonstrating its potential to enhance mine safety management efficiency and accident prevention capabilities.

4.1 Early Warning System for Coal Mine Gas Leakage and Explosion Risks

Gas leakage represents one of the most critical risks in mine safety management, particularly during coal mining operations. Abnormal increases in methane concentrations can directly endanger the lives of personnel and result in significant economic losses. Traditional gas monitoring methods primarily rely on real-time monitoring via single sensors, which, while providing basic alarm functions, lack the comprehensive analytical capability to assess the interplay of multiple factors within complex environments.

An early warning mechanism based on multimodal large models achieves precise identification and prediction of gas leakage risks by integrating data from methane concentration sensors, video surveillance, and historical accident records. For instance, when sensors detect abnormal concentration spikes, the system analyses video footage to assess ventilation conditions, equipment operation, and worker distribution within the mine, thereby determining potential escalation risks. Simultaneously, the system extracts analogous cases from historical accident records and generates tailored warning messages based on current environmental characteristics. For instance, during elevated methane concentrations coupled with abnormal ventilation equipment operation, the system issues alerts such as: 'Methane concentration exceeds permissible limits with inadequate ventilation; immediate personnel evacuation recommended.' This provides mine management with timely decision-making support.

4.2 Monitoring of Operational Personnel Behaviour Violations

Worker non-compliance constitutes a significant contributing factor to mining safety incidents.

Conventional behavioural monitoring methods typically rely on manual inspections or rudimentary video surveillance, proving inadequate for achieving comprehensive coverage and real-time analysis across large-scale operational areas. In contrast, an early warning mechanism based on multimodal large language models can automatically identify worker violations and issue alerts through real-time analysis of video data, integrated with environmental sensor readings and operational log text data.

In practical application, the system can utilise video surveillance data to capture in real time whether personnel are wearing safety helmets, entering hazardous zones, or engaging in other non-compliant operations. Upon detecting abnormal behaviour, the system integrates environmental monitoring data to assess the current operational hazard level and generates corresponding warning messages. For instance, should a worker be observed without a safety helmet while approaching a high-risk zone, the system will generate an alert stating: 'Worker not wearing safety helmet and approaching hazardous area. Correct immediately.' This notification is disseminated via voice broadcast or SMS to relevant supervisors, thereby effectively mitigating safety incidents arising from non-compliance.

4.3 Equipment Operational Status Monitoring and Fault Prediction

The operational status of mining equipment directly impacts production efficiency and operational safety. Equipment failures may not only cause production interruptions but also trigger severe secondary incidents. Traditional equipment monitoring methods typically rely on single-sensor data, lacking comprehensive analytical capabilities regarding equipment operational status. The early warning mechanism developed in this study achieves multidimensional monitoring and fault prediction by integrating equipment operational sensor data, video data, and maintenance log text data.

For instance, when sensors detect abnormal vibrations or elevated temperatures, the system can analyse visual data to assess external changes (such as oil leaks or unusual shaking) alongside historical fault records in maintenance logs to determine potential failure risks. Should the system detect multiple overlapping fault indicators—such as abnormal vibration, excessive temperature, and maintenance records indicating recent similar issues—it generates an alert stating: 'Equipment operation abnormal, potential severe fault risk present. Immediate inspection required.' This enables management to take proactive measures, thereby preventing safety incidents caused by equipment failure.

4.4 Prediction and Early Warning of Mine Collapse Risks

Mine collapses represent another prevalent major safety hazard in mining operations, often arising from multiple factors including geological conditions, equipment vibrations, and operational practices. Conventional collapse risk prediction methods typically rely on geological sensor data, lacking the capacity for comprehensive analysis of other pertinent factors. The early warning mechanism developed in this study achieves multidimensional prediction and alerting of collapse risks by integrating geological sensor data, video surveillance footage, and textual operational log data. In practical application, when geological sensors detect abnormal increases in rock pressure, the system analyses equipment operational status and worker distribution within the mine using video data. It then evaluates historical records from operational logs to assess whether other collapse triggers exist under current working conditions. For instance, upon detecting both elevated rock pressure and intense equipment vibration, the system generates an alert stating: 'Abnormally elevated rock pressure coupled with severe equipment vibration indicates collapse risk. Cease operations immediately.' This warning is presented via a visual interface to mine management personnel, thereby providing timely evacuation guidance for workers.

4.5 Comprehensive Application Value

Analysis of the aforementioned application scenarios demonstrates that the multimodal large-model-based mine safety early warning mechanism holds significant practical value across multiple critical stages of mining operations. Its core advantage lies in comprehensively perceiving the safety conditions of the mining environment, accurately predicting potential risks, and generating specific warning information through the deep integration and intelligent analysis of multimodal data. This not only substantially enhances the efficiency of mine safety management but also effectively reduces casualties and economic losses resulting from safety incidents. Moving forward, the widespread adoption of this mechanism within mining operations will provide robust technical support for the safe production of mining enterprises. Simultaneously, it offers valuable reference points for safety management across other industrial sectors.

5 TECHNICAL CHALLENGES AND OUTLOOK

The design and implementation of a mine safety early warning mechanism based on multimodal large language models has demonstrated its potential and practical value within complex industrial settings. Nevertheless, as the system undergoes progressive development and experimental validation, several issues and challenges warrant further examination. This chapter will explore its technical advantages, limitations in real-world applications, potential avenues for improvement, and future development trends, thereby providing reference for subsequent research and practical implementation.

5.1 Analysis of Technical Advantages

The multimodal large-model-driven mine safety early warning mechanism proposed in this study possesses the following significant advantages:

1) Multimodal data fusion capability

By integrating environmental sensor data, video surveillance footage, textual records and other multimodal information, the early warning mechanism comprehensively perceives dynamic changes within the mining operational environment. Multimodal data fusion not only enhances the ability to supplement deficiencies in single data sources but also identifies potential risk correlations through cross-modal interactive analysis.

2) Cross-modal learning and feature extraction

Large models based on the Transformer architecture efficiently extract features from diverse modalities and achieve deep feature fusion through cross-modal attention mechanisms. This approach effectively overcomes the limitations of traditional single-modal feature extraction and fusion, enabling the model to demonstrate greater robustness and generalisation capabilities in complex scenarios.

5.2 Limitations in practical application

Although this mechanism demonstrated favourable performance in experimental validation, it still faces certain challenges and limitations in practical application:

1) Data Quality and Multimodal Data Imbalance

Data quality in mining environments is frequently compromised by sensor failures, network latency, and harsh environmental conditions, resulting in missing or noisy data. Furthermore, variations exist in the sampling frequency and coverage of different modal data types—for instance, sensor data may be sampled at high frequency while textual records are updated infrequently. Achieving efficient multimodal fusion under such imbalanced data conditions remains a significant challenge.

2) Computational Complexity and Resource Requirements

Training and inference of multimodal large models demand substantial computational resources, particularly when processing high-resolution video data and extensive historical text records, necessitating high hardware performance. Resource-constrained mining enterprises may face significant cost pressures in deploying and maintaining such complex models.

3) Scenario Adaptability and Robustness

Mining environments are complex and variable, with significant differences in geological conditions, equipment types, and operational workflows across distinct mining areas. Although multimodal large models possess a degree of generalisation capability, their robustness requires further enhancement when confronting extreme scenarios within specific contexts—such as complete sensor data loss or video surveillance blind spots.

5.3 Future Development Trends

Research and application of mine safety early warning mechanisms based on multimodal large models remain in their infancy. Future development trends are primarily reflected in the following aspects:

1) Intelligence and Automation

With continuous advancements in artificial intelligence technology, mine safety early warning systems will progressively transition from passive monitoring to active intervention. For instance, upon detecting high-risk events, the system can automatically trigger emergency response plans or control equipment operations, thereby further enhancing safety management efficiency.

2) Integration with IoT and Blockchain Technologies

By integrating with IoT technologies, systems can achieve more efficient data collection and equipment coordination. The incorporation of blockchain technology enhances data credibility and security, providing safeguards for cross-organisational collaboration.

3) Continuous Dynamic Optimisation

As mining operational environments and safety management requirements evolve, systems must possess capabilities for continuous learning and dynamic optimisation. For instance, online learning techniques can be employed to update model parameters in real time, ensuring the system maintains high predictive accuracy and adaptability.

6 CONCLUSION

Mine safety management constitutes a pivotal component in safeguarding the lives of mining personnel and ensuring uninterrupted production operations. Conventional single-modal monitoring approaches frequently struggle to achieve comprehensive perception and precise early warning when confronted with the complex and dynamic conditions inherent in mining environments. The multimodal large-model-based mine safety early warning mechanism leverages the advantages of artificial intelligence in data processing and risk prediction by integrating multimodal information such as sensor data, video surveillance footage, and textual records, thereby providing an innovative solution for mine safety management.

By integrating diverse data sources, this mechanism enables dynamic perception of mining environments within complex scenarios, addressing the limitations of single-modal approaches. Utilising a large model based on the Transformer architecture, it achieves deep fusion and analysis of multimodal features through cross-modal attention mechanisms, delivering efficient risk identification and decision support for safety management in intricate industrial settings.

Whilst this research has yielded significant outcomes, certain limitations persist, including uneven quality of

multimodal data, high computational complexity of the model, and room for improvement in scenario adaptability. Future research directions encompass: optimising data acquisition and processing workflows; developing lightweight models to reduce hardware requirements; enhancing system robustness and adaptive capabilities; and further improving user experience alongside the interpretability of warning information.

Through continuous technological innovation and engineering practice, multimodal large-model-based mine safety early warning mechanisms hold promise to play an increasingly significant role in mine safety management, providing robust safeguards for the safe production of mining enterprises and the health and safety of their personnel.

REFERENCES

[1] Vaswani, A., Shazeer, N., Parmar, N., et al. (2017). Attention is All You Need. Advances in Neural Information Processing Systems (NeurIPS), 30, 5998–6008.

[2] Baltrušaitis, T., Ahuja, C., & Morency, L. P. (2019). Multimodal machine learning: A review and classification. IEEE Transactions on Pattern Analysis and Machine Intelligence, 41(2), 423–443.

[3] Zhang, Z. Q., Han, G., Xu, L., et al. (2021). Deep learning-based safety monitoring and early warning system for underground mines. Safety Science, 139, 105248.

[4] Goodfellow, I., Bengio, Y., & Courville, A. (2016). Deep Learning. MIT Press.

[5] Zhou, B., & Pan, J. (2020). Intelligent Prediction of Coal Mine Risks Based on IoT and Machine Learning. Journal of Cleaner Production, 262, 121233.

[6] Li, Y., Wang, X., Liu, J., et al. (2022). Multimodal Fusion in Industrial Safety Monitoring: Challenges and Opportunities. IEEE Journal of IoT, 9(5), 3391–3406.

[7] Chen, T., & Guestrin, C. (2016). XGBoost: A Scalable Tree Boosting System. Proceedings of the 22nd ACM International Conference on Knowledge Discovery and Data Mining (KDD), 785–794.

[8] He, K. M., Zhang, X., Ren, S. Q., & Sun, J. (2016). Deep residual learning for image recognition. Proceedings of the IEEE Conference on Computer Vision and Pattern Recognition (CVPR), 770–778.

[9] Zhu, J. G., & Wu, X. M. (2023). Applications of artificial intelligence-driven multimodal systems in high-risk industries: The case of mine safety. Industrial Safety and Risk Management, 45(3), 211–225.

[10] Wang Qiang, Li Ming, Zhang Xiaodong. (2021). Research on Mine Safety Monitoring Systems Based on Multimodal Data Fusion. Journal of Safety Science, 31(8), 15–22.

[11] Dosovitskiy, A., Beyer, L., Kolesnikov, A., et al. An Image is Worth 16x16 Words: Transformers for Image Recognition at Scale[C]. International Conference on Learning Representations (ICLR), 2021.

[12] Wu, T., & Chen, Y. (2020). Key technologies and applications for intelligent development in mining[J]. Mining Research and Development, 40(5), 1–6.

An Exploration of Multi-Axis CNC Machining Technology in Automotive Component Processing

Zhuyong Su*

Jingzhou Polytechnic College, Jingzhou, Hubei 434000, China

*Corresponding author, E-mail: 463157894@qq.com

Abstract:

With the rapid advancement of the automotive industry, demands for precision and efficiency in automotive component machining continue to rise. As an advanced mechanical manufacturing method, multi-axis CNC machining technology has gained widespread application in automotive component production due to its high precision, efficiency, and flexibility. This paper outlines the fundamental principles and characteristics of multi-axis CNC machining technology, focusing on its application advantages, key technologies, and practical case studies within automotive component manufacturing. It further explores future development trends. Through this research, the aim is to provide the automotive manufacturing sector with practical guidance on applying multi-axis CNC machining technology, thereby advancing the upgrading and development of automotive component processing techniques.

Keywords:

Multi-axis CNC machining technology; Automotive components; Machining precision; Machining efficiency; Five-axis simultaneous machining

1 INTRODUCTION

With societal progress and the vigorous advancement of science and technology, numerical control technology has achieved deep integration with automotive manufacturing, driving improvements in the precision of automotive component machining. Particularly within modern automotive production, the complexity, diversity, and high-precision requirements of automotive components continue to increase, rendering traditional machining techniques increasingly inadequate for meeting demands for efficient, high-quality production. As an advanced machining method, multi-axis CNC machining demonstrates significant application potential in the field of automotive component processing, owing to its high precision, efficiency, and flexibility.

2 INTRODUCTION TO MULTI-AXIS CNC MACHINING TECHNOLOGY

2.1 Definition and Characteristics

Multi-axis CNC machining technology refers to the use of multiple axes on a single machine tool for digital control, enabling the processing of complex workpieces. This technology is typically employed on five-axis or

higher CNC machine tools, with some high-end machines achieving nine-axis or greater control capabilities. Characterised by high precision, multi-axis CNC machining facilitates the high-accuracy processing of workpieces with complex geometries. It finds extensive application across sectors including aerospace, medical devices, energy, and automotive manufacturing.

2.2 Fields of application

In terms of application domains, multi-axis CNC machining technology boasts an extensive scope of utilisation. Within the automotive manufacturing sector, it finds application in the high-precision machining of automotive components, engine cylinder blocks, and turbochargers. Within aerospace, the machining of complex components like aircraft engine blades, propellers, and nacelles also necessitates multi-axis CNC machining. Furthermore, this technology plays a vital role in medical devices and energy sectors, including the production of artificial joints, bone pins, dental implants, wind turbine blades, and nuclear power plant components.

3 ADVANTAGES OF MULTI-AXIS CNC MACHINING TECHNOLOGY IN AUTOMOTIVE COMPONENT PRODUCTION

3.1 Excellent capability for machining complex geometries

Compared to manual and conventional control operations, multi-axis CNC machining technology offers significant advantages in the processing of automotive components. Automotive parts often feature complex geometries, particularly for critical components such as engine cylinders, crankshafts, and turbochargers, which present considerable manufacturing and machining challenges. Multi-axis CNC machining excels at processing intricate geometries, accommodating diverse component requirements. For instance, in engine cylinder production, this technology precisely controls the contours of combustion chambers, intake ports, and exhaust ports, enhancing combustion efficiency within the engine cavity. In crankshaft machining, it enables complex surface processing and accurate weight-reduction hole drilling, improving crankshaft balance and service life.

3.2 Enhance machining precision

Multi-axis CNC machining technology is applied in multi-axis CNC machine tools, which possess exceptionally high positioning accuracy, enabling strict control of precision standards in automotive component processing. Through simultaneous control of multiple axes, these machine tools achieve precise regulation of tool movement trajectories, thereby significantly enhancing the machining accuracy of automotive components. This high-precision processing not only ensures component quality but also contributes to extending vehicle service life while improving overall performance and reliability.

3.3 Reduce processing steps

Through the application of multi-axis CNC machining technology, each automotive component can undergo multi-surface machining operations in a single setup during manufacturing and processing. This reduces machining stages, enhances processing efficiency, and elevates the overall production standards of the workshop. Traditional machining methods often necessitate multiple clamping and positioning operations, which can lead to machining errors and increased processing time. Multi-axis CNC machining, however, accomplishes multi-surface machining with a single clamping operation. This effectively eliminates

positioning errors and time wastage associated with repeated clamping, thereby enhancing both production efficiency and machining quality.

3.4 Save materials and energy

With the support of multi-axis CNC machining technology, material wastage in automotive component manufacturing and processing has been effectively controlled. Through digitalised management, material application planning has been refined, contributing to enhanced material utilisation efficiency. Concurrently, multi-axis CNC machining enables high-precision processing, thereby reducing material wastage caused by machining errors. Furthermore, the high-efficiency machining capabilities of multi-axis CNC machine tools also help minimise energy consumption, promoting sustainable development within the automotive manufacturing sector.

3.5 Enhance production flexibility

Through programming, multi-axis CNC machining centres can execute diverse machining instructions, facilitating adaptation to the varied production demands of automotive components. This manufacturing flexibility enables the automotive industry to swiftly adjust production schedules and product ranges in response to market fluctuations. For instance, during the development of new vehicle models, multi-axis CNC machining technology can rapidly accommodate design modifications and shifting machining requirements, thereby shortening product development cycles and time-to-market whilst enhancing corporate competitiveness.

3.6 Enhance product competitiveness

Supported by advanced technologies such as multi-axis CNC machining, the automotive manufacturing industry continues to evolve, ensuring the processing quality of its products while continuously enhancing their value-added attributes. Against this backdrop, the competitiveness of automotive products in the marketplace will steadily increase, effectively safeguarding consumer rights. High-quality, high-performance automotive components not only elevate the overall performance and reliability of vehicles but also bolster consumer recognition and loyalty towards automotive brands, thereby strengthening the market competitiveness of automotive products.

4 KEY TECHNOLOGIES IN MULTI-AXIS CNC MACHINING AND THEIR APPLICATION IN AUTOMOTIVE COMPONENT PROCESSING

4.1 Five-axis machining technology

1. Technical Principles and Advantages

Five-axis machining technology represents an advanced CNC processing method, enabling simultaneous control of the tool across five axes to achieve precision machining operations on components. Specifically, the five axes comprise three linear axes (X, Y, Z) for translational movement and two rotary axes (A, B). Under programme control, this ensures greater precision in the tool's motion trajectory. The technology's advantage lies in its capability to machine components of exceptionally complex geometries, such as engine cylinders, crankshafts, and automotive turbochargers.

2. Application Cases in Automotive Component Machining

（1）Engine cylinder machining

In the machining of engine cylinders, operators can utilise five-axis machining centres to precisely control the shape of the cylinder bore. Particular attention must be paid to ensuring programme accuracy during the machining of critical areas such as the combustion chamber, intake duct, and exhaust duct. Effective shape control enhances combustion efficiency within the engine's internal cavities. Cylinder walls also require intricate structures such as fuel injection ports and spark plug holes. The positioning and orientation of these apertures often present significant complexity, necessitating the precision machining capabilities afforded by five-axis machining technology.

（2）Automotive crankshaft machining

During the machining of automotive crankshafts, five-axis machining technology can be employed to achieve complex surface machining and the processing of weight-reduction holes. In complex surface machining, this technology enables the completion of operations on surfaces such as the main journals and connecting rod journals within a single setup, thereby enhancing machining efficiency and precision. For weight-reduction hole machining, this technology precisely forms these holes according to their required shape and position, thereby reducing crankshaft mass and ensuring component balance.

（3）Turbocharger machining

The blades of turbochargers typically feature complex spatial curved surfaces. By enhancing boost efficiency and reducing noise levels, the application of five-axis machining technology ensures precise control over the shape of these blades. Furthermore, the bearing housings of turbochargers also exhibit intricate geometries. To guarantee stable bearing operation, five-axis machining technology is required for the precise machining of these housings.

4.2 Numerical Control Programming and Simulation Technology

1. Numerical Control Programming Technology

Advanced CNC programming software can generate complex machining programmes, which are validated and optimised through simulation technology to enhance the efficiency and safety of automotive component processing. Automated precision machining operations on multi-axis CNC machine tools necessitate the use of software such as CAD/CAM. Technicians employ CAD software to design three-dimensional models of components, subsequently utilising CAM software to generate machining programmes. These programmes are then implemented into multi-axis CNC machine tools to achieve automated precision operations on automotive components. Within CAM software, operators may also directly write G-codes and M-codes to optimise the management of machining programmes for CNC machines. Furthermore, CAM software's automatic programming capabilities can be utilised to generate machining programmes autonomously based on the part's geometry and processing requirements.

2. Simulation and Collision Detection Technology

With the aid of CNC technology, technicians can conduct simulation modelling during the machining of automotive components to detect collisions between cutting tools and fixtures, thereby ensuring the safety of the machining process. Through simulation, tool paths can be optimised, helping to reduce idle travel and enhance machining efficiency. Furthermore, simulation testing enables optimised control of cutting parameters for different tools—such as rational management of cutting speed, feed rate, and cutting depth—to identify optimal parameter combinations for precision machining of automotive components. Taking automotive gearbox machining as an example: during the design phase, CAD software can be employed to

create a three-dimensional model of the gearbox housing, achieving precise modelling of internal spatial layout, hole positions, and threading. During the programming phase, the completed CAD model is imported into CAM software for cutting parameter optimisation. The simulation stage involves collision detection, with toolpaths refined according to transmission machining requirements to enhance efficiency and surface finish. In the machining phase, the generated program is transferred to CNC machine tools for execution.

4.3 Error compensation technology

1. Technical Principles

In multi-axis CNC machining of automotive components, errors may arise from systematic deviations and cutting forces. Through error compensation techniques, these discrepancies can be mitigated, thereby reducing their impact on component machining accuracy and enhancing overall processing quality. Specifically, error compensation within multi-axis CNC machining constitutes a method employing software algorithms to rectify deviations arising during actual machining operations. The occurrence of machining errors stems from multiple factors, including inherent manufacturing tolerances of the machine tool itself, thermal deformation, tool wear, and workpiece clamping inaccuracies.

2. Applications in Automotive Component Machining

（1）Machine Tool Error Compensation

Through error compensation software provided by machine tool manufacturers, linear errors, rotational errors, thermal deformation errors and other factors are compensated for, thereby enhancing the machine tool's overall machining accuracy. Particularly when machining automotive components with stringent precision requirements, the application of machine tool error compensation technology can significantly improve machining accuracy.

（2）Tool wear compensation

During machining operations, cutting tools on machine tools gradually wear down, which can also lead to a decline in the machining accuracy of components. Through error compensation technology, the wear condition of machine tool cutting tools can be monitored, enabling technicians to adjust machining parameters at any time to compensate for machining errors caused by tool wear.

（3）Workpiece clamping error compensation

During workpiece clamping, clamping errors may arise due to imprecise fixtures or workpiece deformation. The application of error compensation technology enables automatic correction of the workpiece during machining by adjusting the machining path, thereby mitigating the impact of clamping errors on machining accuracy.

（4）Dynamic error compensation

During the machining of automotive components, dynamic machining errors may arise due to vibrations and friction occurring in the machine tools. To address this, error compensation technology can be employed to continuously monitor the dynamic response of the machine tools and dynamically adjust machining parameters, thereby ensuring the precision of component machining.

（5）Thermal deformation error compensation

Machine tools are susceptible to temperature fluctuations during machining operations, which can cause thermal deformation of components and result in significant machining errors. Consequently, error compensation technology must be employed to continuously monitor temperature variations within the machine tool, thereby preventing deformation errors from adversely affecting the machining quality of components.

5 PRACTICAL APPLICATIONS OF MULTI-AXIS CNC MACHINING TECHNOLOGY IN AUTOMOTIVE COMPONENT PRODUCTION

5.1 Case Study: Huazhong CNC and Dongfeng Equipment Manufacturing Plant Collaboration

Wuhan Huazhong CNC Co., Ltd. (hereinafter referred to as Huazhong CNC) has joined forces with Dongfeng Equipment Manufacturing Plant to mass-produce high-precision four-axis horizontal machining centres equipped with Huazhong CNC's HNC-818B high-performance CNC system. Tailored to meet the CNC machining demands for critical components of passenger car engines, these centres form a flexible production line successfully deployed at a major domestic automotive manufacturer. This flexible production line for passenger car engines possesses capabilities for high-speed multi-surface milling, boring, drilling, and tapping, making it particularly well-suited for processing cast iron components such as cylinder blocks and cylinder heads. Currently, the high-precision four-axis horizontal machining centres jointly produced by HNC and Dongfeng Equipment Manufacturing Plant have achieved batch production for Complementary production, are operating in excellent condition, and have received favourable feedback from users.

1. Machine Tool Performance Parameters High dynamic performance: Maximum linear axis acceleration of 1g, feed rate of 20m/min, rapid traverse of 60m/min. High machining precision: Positioning accuracy up to 5μm, repeat positioning accuracy up to 3μm, milled hole cylindricity within 10μm (hole diameter 100mm). High-Performance Spindle Configuration: Features an electric spindle with 25kW power and maximum speed of 8000 r/min. Hydraulic Locking Turret: Enhances machining efficiency while maintaining heavy-cutting precision during ø120 peripheral milling operations. Dual control panels: The machining position panel controls machine parameters, programmes, and operations, while the front panel manages workpiece handling. The system automatically loads the current workpiece programme. Tool breakage detection: A servo-driven inspection unit at the front of the overhead tool magazine assesses tool integrity before changes or post-machining, ensuring product quality compliance.

2. CNC System Solutions Primary Functions: The four-axis horizontal machining centres manufactured by Dongfeng Equipment Manufacturing Plant primarily utilise the high-speed, high-precision machining capabilities of the HNC-818B CNC system from Huazhong CNC. These centres feature three-axis and four-axis interpolation capabilities, online tool and workpiece measurement, spatial error compensation and fully closed-loop control functionality, fully open network interfaces compatible with smart production lines (expandable to EtherCAT bus communication protocols), and advanced control features including machining big data collection and monitoring.

5.2 Case Study: Collaboration between Huazhong CNC and Beijing Industrial Research Precision Machinery Co., Ltd.

Huazhong CNC has established a close collaboration with Beijing Gongyan Precision Machinery Co., Ltd. to address the automotive industry's demand for CNC machining of critical engine components. This partnership has resulted in the mass production of the μ2000/630HF precision four-axis horizontal machining centre, equipped with Huazhong CNC's high-end HNC-848C CNC system. Currently, the jointly produced precision four-axis horizontal machining centres have achieved volume sales. Primarily employed for machining high-precision components such as powertrain housings and cylinder blocks, they are well-suited for both multi-variety and high-volume production.

1. Machine Tool Performance Parameters Machine Tool Structure: Features a T-shaped layout with a gantry frame structure. The Z-axis employs dual-drive technology to enhance dynamic rigidity, rapidly suppress

vibrations, and improve machined surface quality. The Y-axis incorporates a weight-balanced headstock design to ensure excellent dynamic performance. The foundation components utilise high-quality cast iron, endowing the machine tool with high rigidity, precision, and superior dynamic characteristics. Working Range: Machine table dimensions 630x630mm, XYZ-axis travel 1000/900/900mm. Spindle Configuration: Spindle speed 8000 r/min, rapid traverse 30m/min, linear axis positioning accuracy 0.006mm, repeatability 0.0035mm, rotary table positioning accuracy 6', repeatability 3'.

2. Application Results The μ2000/630HF horizontal machining centre, equipped with the HNC-848C CNC system from Huazhong CNC, has been deployed in batch production at an automotive gear transmission company. It is primarily utilised for the efficient, high-precision machining of medium-to-heavy-duty automotive transmission housing components, meeting the user's processing requirements.

6 CHALLENGES AND COUNTERMEASURES IN THE APPLICATION OF MULTI-AXIS CNC MACHINING TECHNOLOGY FOR AUTOMOTIVE COMPONENT PROCESSING

6.1 Application Challenges

1. Technical Complexity Multi-axis CNC machining technology involves the simultaneous control of multiple axes, resulting in complex processing procedures that demand high technical proficiency from programmers. Furthermore, the commissioning and maintenance of multi-axis CNC machine tools necessitate operation by specialised technical personnel.

2. High Equipment Costs Multi-axis CNC machine tools typically command a premium price, presenting significant financial strain for some small and medium-sized enterprises when considering acquisition. Additionally, maintenance and servicing costs for such equipment remain comparatively substantial.

3. Balancing Machining Efficiency and Precision Within multi-axis CNC machining, achieving a balance between enhancing machining efficiency while maintaining precision presents a key challenge. Excessively high machining speeds may compromise dimensional accuracy, whereas excessively low speeds adversely affect production throughput.

6.2 Countermeasures

1. Enhancing Technical Training Given the complexity of multi-axis CNC machining technology, automotive manufacturers should intensify training for technical personnel to elevate their programming and operational proficiency. Concurrently, external specialists may be engaged to provide technical guidance and training, thereby enhancing overall technical capabilities.

2. Optimising Equipment Configuration Automotive manufacturers should rationally configure multi-axis CNC machine tools according to their production requirements and financial circumstances. Equipment costs may be reduced and utilisation rates improved through leasing or equipment sharing arrangements. Furthermore, collaboration with equipment manufacturers to co-develop multi-axis CNC machines tailored to enterprise requirements should be considered.

3. Develop Efficient Machining Strategies To address the balance between machining efficiency and precision, automotive manufacturers may partner with research institutions to develop high-efficiency machining strategies. Optimising toolpaths, cutting parameters, and machining sequences can enhance both efficiency and accuracy. Simultaneously, simulation technologies can predict and refine machining processes, thereby reducing trial-and-error costs and time.

7 PROSPECTS FOR THE APPLICATION OF MULTI-AXIS CNC MACHINING TECHNOLOGY IN AUTOMOTIVE COMPONENT PROCESSING

7.1 Technological Development Trends

1. Enhanced machining precision As automotive industry demands for component accuracy intensify, multi-axis CNC machining technology will evolve towards greater precision. This encompasses more accurate tool positioning, more stable machine tool control, and more effective error compensation techniques. In the future, multi-axis CNC machining is anticipated to achieve nanometre-level precision, meeting the growing need for higher-accuracy automotive component fabrication.

2. More Complex Machining Tasks As automotive designs continually innovate, multi-axis CNC machining technology will need to handle increasingly complex machining tasks. This encompasses more intricate geometries, smaller machining dimensions, and more precise surface quality requirements. In the future, multi-axis CNC machining technology will continually expand its application scope to meet the diverse machining demands of automotive components.

3. Faster Machining Speeds To enhance production efficiency, multi-axis CNC machining technology will require achieving higher machining speeds. This encompasses more efficient toolpath planning, faster machine tool movements, and optimised cutting parameter settings. In the future, multi-axis CNC machining technology is expected to combine high-speed machining with high efficiency, thereby improving the production efficiency of automotive components.

4. More Intelligent Machining Systems With advancements in artificial intelligence and machine learning, multi-axis CNC machining systems will become increasingly intelligent. This will encompass more sophisticated machining strategies, smarter toolpath optimisation, and greater automation in quality control. Future systems are anticipated to incorporate adaptive machining and intelligent monitoring capabilities, thereby elevating both the machining quality and production efficiency of automotive components.

5. More Environmentally Friendly Machining Processes The automotive manufacturing sector faces environmental and sustainability challenges. Multi-axis CNC machining technology must evolve towards more eco-conscious processes. This entails employing more sustainable tool materials, more efficient coolants, and more energy-efficient machine tool designs. Future advancements will focus on reducing waste emissions and energy consumption during machining, thereby advancing sustainable development within the automotive manufacturing industry.

7.2 Market Prospect Analysis

With the continuous advancement of the automotive industry and consumers' increasing demands for vehicle quality, multi-axis CNC machining technology holds promising prospects for application in automotive component manufacturing. On the one hand, automotive manufacturers will intensify investment and research efforts in multi-axis CNC machining technology to enhance the precision and efficiency of component production. On the other hand, as this technology matures and becomes more widespread, its application will progressively extend to a broader range of automotive component machining. Furthermore, with the continuous expansion of domestic and international automotive markets and intensifying competition, multi-axis CNC machining technology will become a crucial means for manufacturers to bolster product competitiveness and market share.

8 CONCLUSION

Multi-axis CNC machining technology holds significant application value in the processing of automotive components. By introducing the fundamental principles and characteristics of this technology, this paper analyses its application advantages, key technologies, and practical case studies within automotive component manufacturing. Concurrently, it proposes corresponding strategies to address challenges encountered in its implementation, while also outlining future development trends and market prospects. It is foreseeable that in future development, multi-axis CNC machining technology will play an increasingly vital role in the automotive component manufacturing sector, driving the advancement and evolution of the automotive manufacturing industry.

REFERENCES

[1] Yang Wenping. Research on the Application of CNC Technology in Automotive Component Machining [J]. Automotive Maintenance Technician, 2024(20):123-125.

[2] Ma Yuliang, Liang Haihua. Application of Multi-Axis CNC Machining Technology in Automotive Component Processing [J]. Science and Technology Information, 2024(18):105-107,123.

[3] Song Hui. Application of CNC Technology in Mechanical Processing of Automotive Components [J]. Automotive Testing Report, 2024(8): 62-64.

[4] Ma Chunxin. Research on the Application of Multi-Axis CNC Machining Technology in Automotive Component Processing [J]. Internal Combustion Engines and Accessories, 2024(7): 128-130.

[5] Jin Bin. Analysis of Multi-Axis CNC Machining Technology in Automotive Component Processing [J]. Modern Manufacturing Technology and Equipment, 2024(5):120-122.

[6] Cao Zhuming, Feng Zhixin, Gu Chunguang, Jia Junliang, Zhang Yabiao. Research on Multi-Axis Machining of Complex Parts for a Convex Roller [J]. Mechanical Engineer, 2020(11):102-104.

[7] Liu Yanshen. Application of UG Variable-Axis Contour Milling in Complex Surface Machining [J]. Automation Technology and Application, 2016, 35(6):37-40.

[8] Shen Yong, Guo Hui, Fan Zhimin, Yue Linfeng. 3+A Variable Profile Milling for Surface Machining [J]. Mechanical Engineer, 2016(4):198-199.

[9] Fan Zhimin, Guo Hui, Xu Fengguo, Yue Linfeng. Four-Axis Surface Milling Machining [J]. Mechanical Engineer, 2017(1): 240-241.

[10] Jin Xia. Research on Variable-Axis Surface Contour CNC Milling Based on UG/CAM Module [J]. Electromechanical Product Development and Innovation, 2008, 21(2): 179-180.

[11] Yang Jun. Exploration of UG NX Component Geometric Modelling [J]. Heilongjiang Science and Technology Information, 2015(23):36.

[12] Li Yanxia. Application Research on CNC Milling Programming and Simulation Based on UG [J]. Coal Mining Machinery, 2010, 31(5):113-116.

[13] Dong Guangqiang. Optimisation Study of Parameters for CNC Milling Processing Based on UG [J]. Machine Tools and Hydraulics, 2012, 40(3): 80-83.

[14] Wang Suyu, Jiang Bin. Surface Design and CNC Machining Simulation Based on UG [J]. Coal Mining Machinery, 2013, 34(2): 141-143.

Design and Practice of Integrating Large Models with Low-Code Platforms

Pan Luo*,Jiaojiao Wan

Wuhan Yishikong Technology Co., Ltd., Wuhan, Hubei 430000, China

*Corresponding author, E-mail: 369141562@qq.com

Abstract:

With the rapid advancement of artificial intelligence technology, Large Language Models (LLMs) have gradually become a significant driving force in the intelligentization of software development. Meanwhile, low-code platforms have gained widespread adoption in enterprise information system construction due to their rapid development capabilities and ease of use. However, existing low-code platforms still exhibit limitations in terms of flexibility and intelligence. To address these issues, this paper proposes an intelligent development tool that integrates large language models with low-code platforms. Leveraging the natural language understanding and code generation capabilities of large language models, this approach significantly enhances the intelligence of low-code platforms. The paper elaborates on the design principles, key technical implementations, and practical application effects of the proposed intelligent development tool. Furthermore, the effectiveness of this method is validated through practical case studies.

Keywords:

Large Model; Low-Code Platform; Intelligent Development; Code Generation; Natural Language Processing (NLP)

1 INTRODUCTION

In recent years, as digital transformation has deepened, enterprises have increasingly demanded greater efficiency and flexibility in software development. Low-code platforms, renowned for their rapid development speed and user-friendly operation, have emerged as a key choice for corporate digitalisation initiatives. The 2025 Government Work Report explicitly states that efforts will continue to advance the 'AI Plus' initiative, promoting the deep integration of digital technologies with manufacturing and market strengths, while supporting the application of large models across broader domains. Furthermore, the draft National Economic and Social Development Plan for 2025 emphasises increased investment in artificial intelligence, driving technological innovation and industrial implementation of large language models. However, traditional low-code platforms still face limitations in functional scalability and intelligent development assistance. Concurrently, the rapid advancement of large language model technology has opened new avenues for intelligent software development. How to leverage large language models to enhance the intelligence of low-code platforms has thus become a critical research focus. With the rapid advancement of artificial intelligence technology, large language models (LLMs) have demonstrated immense potential in the software development domain. Concurrently, low-code platforms, owing to their convenience and efficiency, have progressively become vital tools supporting enterprise digital transformation. Nevertheless, traditional low-code platforms exhibit shortcomings in intelligent development assistance, flexibility, and support for

complex business operations. This paper proposes an intelligent development tool that deeply integrates LLM technology with low-code platforms. Through techniques such as natural language understanding, intelligent code generation, and component recommendation, it significantly elevates the intelligence level of low-code platforms. It details the technical architecture, functional module design, and key implementation of this intelligent development tool, validating its effectiveness and feasibility through practical project case studies. Additionally, it proposes an LLM-enhanced low-code development architecture (LLM4LC), which overcomes the logical expression limitations of traditional low-code platforms by constructing a three-tier cognitive reasoning engine. Experiments demonstrate that this architecture substantially improves the efficiency of converting business requirements into executable systems. Key components include: 1) a multimodal requirements parser; 2) a dynamic domain adaptation layer; and 3) a security-enhanced code generator. The system has achieved commercial deployment in the government sector, supporting the construction of over 100 pages daily.

2 RESEARCH OVERVIEW

2.1 Research Background

Industry pain points: Traditional low-code platforms suffer from limitations in logical expression capabilities (only capable of handling 30% of complex business scenarios) and high domain adaptation costs (new business module development requiring 2-4 weeks) [5]. Technical breakthrough: The complementary nature of large models like GPT-4 and DeepSeek—demonstrating code generation capabilities (67% pass rate on HumanEval tests)—with low-code visual configuration.

2.2 Innovative Contributions

Proposing a cognitive enhancement code generation paradigm (CogCode) to achieve a three-stage mapping: natural language requirements → visual components → executable code.

Constructing a domain knowledge distillation framework, which enhances the code generation accuracy of foundational models in specific business scenarios by 41.2% through few-shot fine-tuning [6].

Designing a security sandbox mechanism to effectively intercept potential malicious code injection risks.

3 TECHNICAL ARCHITECTURE DESIGN
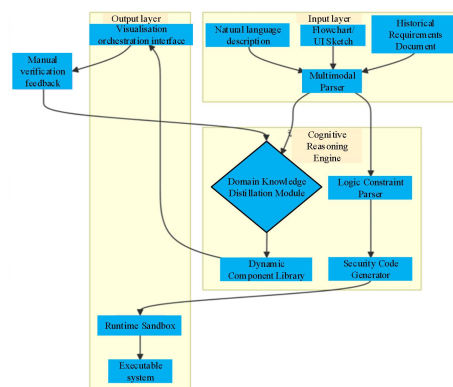
3.1 Overall System Architecture

Figure 1：Overall system architecture diagram

The system's overall architecture comprises three principal components:

1) Input Layer: Receives diverse input data.

2) Cognitive Reasoning Engine: The core processing module responsible for parsing, reasoning, and generation.

3) Output Layer: Generates the final executable system while supporting manual feedback.

The Input Layer consists of data from three distinct sources:

Natural Language Descriptions: Users articulate requirements in natural language, e.g., 'I require an online shopping system.'

Flowcharts/UI Sketches: User-provided flowcharts or interface sketches, which may be hand-drawn or generated by design tools.

Historical Requirement Documents: Existing requirement documents or reference materials from similar projects.

These inputs are processed through a multimodal parser. The role of the multimodal parser is to convert inputs of different forms (natural language, graphical descriptions, historical documents) into a unified internal representation for use by subsequent modules.

Cognitive Reasoning Engine: This constitutes the system's core component, comprising the following modules:

Domain Knowledge Distillation Module: Extracts domain-relevant knowledge from information processed by the multimodal parser. Integrates with the domain knowledge repository for dynamic updating and optimisation. Generates a dynamic component library containing reusable modules, elements, or code snippets.

Logical Constraint Parser: Analyses logical relationships and constraints within inputs, such as business logic and user permissions. Outputs to the secure code generator to ensure generated code adheres to logical constraints and remains secure and reliable. Dynamic Component Library and Secure Code Generator: The dynamic component library provides reusable components for subsequent visual interface orchestration. The secure code generator produces code compliant with security standards, mitigating potential vulnerabilities.

Output Layer: The output layer constitutes the system's final deliverable, comprising the following modules.

Visualisation Orchestration Interface: Generates a visual interface based on the dynamic component library, enabling users to intuitively view and adjust system designs.

Runtime Sandbox: Executes generated code within an isolated environment, ensuring secure and expected behaviour.

Executable System: Ultimately outputs a directly executable system, such as a complete software application or service.

Manual Verification Feedback: Users may manually verify and provide feedback on the visual orchestration interface. This feedback flows back to the domain knowledge distillation module to refine the dynamic component library and subsequent generation logic.

This architecture describes a highly automated, intelligent system designed to parse requirements from diverse inputs and generate final executable systems, while supporting human feedback for optimisation.

Key highlights of the entire process include:

1) Multimodal input support (natural language, sketches, historical documents).

2) Cognitive reasoning engine for domain knowledge extraction and logical analysis.

3) Output phase incorporates manual verification and feedback loops to continuously enhance system performance.

3.2 Multimodal Requirement Parser

3.2.1 Cross-modal alignment model

1)Improved CLIP Architecture

Employing ViT-L/14 as the visual encoder and RoBERTa-large as the text encoder [7]. Cross-modal attention formula:

$$\text{Attention}(Q, K, V) = \text{softmax}\left(\frac{QK^T}{\sqrt{d_k}}\right)V$$

Q (Queries) in the formula: Represents the query vector at the current time step or for the current input. This typically originates from the output of the text encoder. K (Keys) in the formula: Represents the key vector associated with the input data. This may be considered a representation linked to specific image features. V (Values) in the formula: Represents the value vector associated with the key vector, determining the final output returned to the model. The three pivotal elements within the cross-modal attention mechanism: Query, Key, and Value. This formula systematically defines how features are extracted from text and images and utilised for cross-modal tasks. By transforming textual and image features into Q, K, and V respectively, the model effectively distinguishes and leverages information from both modalities, thereby enhancing its performance in multimodal tasks.

1)Adaptive Weight Allocation

Introducing a gating mechanism to dynamically adjust the contribution of multimodal features [8]:

$$g = \sigma\left(W_g[E_{\text{text}}; E_{\text{image}}]\right)$$

$$E_{\text{fused}} = g \cdot E_{\text{text}} + (1 - g) \cdot E_{\text{image}}$$

In the formula, g represents a threshold value computed via a sigmoid function (σ). This sigmoid function maps its input to values between 0 and 1, indicating the relative importance of text and image.

In the formula, W_g denotes a weighting matrix that is multiplied by the concatenated result of the text embedding E_{text} and the image embedding E_{image}. This design enables the model to learn the importance of input modalities, thereby dynamically adjusting its weights.

The fusion result E_{fused} in the formula favours image features when g approaches zero. This weighted averaging method effectively integrates information from both modalities. The gating mechanism adaptively adjusts feature importance, thereby enhancing the model's overall performance.

This adaptive gating mechanism dynamically adjusts the contribution ratio of textual and visual information, enabling better capture of their interrelationships and improving the performance of multimodal learning models. When tackling complex cross-modal tasks such as image-text matching or image caption generation, this flexible weight allocation proves crucial to model effectiveness.

Adaptive weight distribution finds extensive application in the convergence of computer vision and natural language processing. For instance, in tasks like image-text matching or image caption generation, dynamically adjusting modal weights enables models to more effectively comprehend and generate contextually relevant information.

3.2.2 Cross-modal alignment model

Generation of structured requirement descriptions, designed using a domain-specific language (DSL) based on the JSON Schema specification. For example:

```
{
  "form": {
    "labelCol": 6,
    "wrapperCol": 12
```

```
    },
  "schema": {
    "type": "object",
    "properties": {
      "43y1uj2k5e6": {
        "x-decorator": "FormItem",
        "x-component": "PageModel",
        "x-validator": [],
        "x-component-props": {
          "outerId": "1785212260029902850",
          "extraStyle": "color:blue;"
        },
        "x-decorator-props": {},
        "x-designable-id": "43y1uj2k5e6",
        "x-index": 0,
        "_randomValueForUpdate": 0.12138395486446818,
        "x-reactions": {
          "dependencies": [
            {
              "property": "value",
              "type": "any"
            }
          ]
        },
        "description": ""
      }
    },
    "x-designable-id": "y5ixw8i8akd"
  }
}
```

Employing a component-based approach, each page unit is mapped to a designated component. Through the combination and nesting of different components, the final page's visual representation is achieved. A standard event mechanism is provided externally, with all interactive behaviours implemented via an event registration pattern.

4 SECURITY-ENHANCED CODE GENERATION

4.1 Code auto-generation

Based on low-code design patterns and over twenty low-code project case studies, model training has been completed. Upon finalising data models and ER model designs, the model can automatically generate page and form models through product design specification documents. This encompasses capabilities including visual page construction, page scripting, interactive event configuration, and cloud function scripting. Design deliverables undergo acceptance testing by quality assurance personnel, with feedback on identified issues achieving the effect of manual verification.

4.2 Static Analysis Engine

The static analysis engine scans source code without executing it. It identifies security vulnerabilities or quality issues by analysing patterns within the code. The static analysis engine converts code into an abstract syntax tree (AST), a tree structure that better represents the logical relationships within the code. The engine traverses this AST, applying predefined detection rules to identify issues in the code. An AST rule library has been constructed, encompassing 210 vulnerability and quality patterns. This not only identifies errors and vulnerabilities within the code but also enhances the overall security and quality of the code. Key detection rules are illustrated below:

```
class SQLInjectionDetector:
    patterns = [
        r"execute\(.*?['\"]\s*\+\s*[\w]+\)",
        r"format\(.*?%s.*?\)"
    ]

    def scan(self, code):
        violations = []
        for node in ast.walk(parse(code)):
            if isinstance(node, ast.Call):
                for pattern in self.patterns:
                    if re.search(pattern, unparse(node)):
                        violations.append(node.lineno)
        return violations
```

4.3 Dynamic Sandbox Design

A dynamic sandbox constitutes an isolated execution environment, permitting code to run within a controlled virtualised setting to prevent impact on the host system. The design of dynamic sandboxes typically incorporates the following core characteristics:

1) Isolation: Code within the sandbox operates in isolation from the host system, preventing malicious or erroneous code from affecting the host environment.

2) Dynamicity: The sandbox dynamically configures resources such as memory, CPU, and network access permissions according to requirements.

3) Monitoring and Auditing: The sandbox continuously monitors code execution behaviour in real-time and logs activities, facilitating debugging and issue tracing.

When integrating large language models with low-code platforms during code generation, the sandbox serves the following purposes:

1) Security: When executing code generated by large language models, the dynamic sandbox prevents potential security vulnerabilities from compromising the system.

2) Verification: The sandbox environment validates the correctness and functionality of generated code, ensuring it meets expectations.

3) Multi-language Support: The sandbox supports multiple programming languages and frameworks, facilitating developer testing of diverse code types. In this implementation, hardware-level isolation was achieved using Kata Containers [9]. An example resource restriction policy is as follows:

```
resources:
 limits:
```

```
    cpu: "2"
    memory: 4Gi
  requests:
    cpu: "0.5"
    memory: 1Gi
 securityContext:
  readOnlyRootFilesystem: true
```

5 Experiments and Evaluation

5.1 Cross-domain validation experiments

The results of the verification experiments are shown in Table 1.

Table 1 System generation accuracy test

Test Scenario	Complexity of requirements	Generation accuracy/%	Execution success rate/%
Large-screen monitoring system	High (nested conditions exceeding five layers)	95.70	98.20
Administrative Approval Process	China (parallel approval node)	89.30	96.50
Medical Consultation System	High (time-dependent)	82.10	93.80

5.2 Performance Stress Testing

The results of the stress test are shown in Table 2.

Table 2 System performance stress testing

Number of concurrent users	Average response time/s	error rate /%
100	1.2	0.01
500	2.8	0.87
1000	4.5	1.5

6 ENGINEERING PRACTICE CASE STUDIES

Taking the development of a municipal smart property management system as a practical case study, the application was constructed using the intelligent development tools proposed in this paper. The results demonstrate:

1) The project, initially scheduled for a six-month development cycle based on experience, was completed in just 2.5 months using this approach. Development efficiency increased by approximately 60%, with the cycle

shortened by more than half;

2) User learning costs were significantly reduced, enabling even junior developers to become proficient rapidly;

3) System flexibility and intelligence levels were markedly enhanced, strengthening its capacity to meet complex business requirements.

7 CONCLUSION AND OUTLOOK

This paper addresses the shortcomings of current low-code platforms in intelligent development by proposing a novel intelligent development tool that integrates large-model technology with low-code platforms. Through establishing a four-tier technical architecture comprising the user interaction layer, intelligent processing layer, low-code platform layer, and infrastructure layer, it achieves key functionalities such as natural language requirement parsing, intelligent code generation, and intelligent recommendations. Practical case studies demonstrate that this tool effectively enhances the intelligence of low-code platforms, significantly boosts development efficiency, lowers the technical threshold for developers, and meets enterprises' increasingly complex business requirements. During practical application, this intelligent development tool exhibits distinct advantages: Firstly, development efficiency improves by approximately 60%, markedly shortening development cycles and enabling enterprises to respond more swiftly to market demands. Secondly, natural language interaction reduces developers' learning curve, enabling non-professional developers to quickly get up to speed and achieve seamless integration between business requirements and technical implementation. Furthermore, the introduction of intelligent recommendation features has effectively enhanced the development experience and component reuse rate, further improving software quality and stability. Nevertheless, the intelligent development tool proposed in this paper still has certain limitations and room for improvement, warranting further in-depth research. Future research directions could focus on the following aspects:

Firstly, further optimise the deep integration between large language models and low-code platforms. While the current technical architecture has achieved preliminary convergence, there remains scope for improvement in model inference efficiency, real-time responsiveness, and resource consumption. Future exploration should focus on lighter-weight model architectures or model compression techniques to enhance inference efficiency, reduce deployment costs for large models, and elevate the system's real-time interactive capabilities.

Second, expand the application scenarios of intelligent development tools. Current implementation cases primarily focus on approval-based business systems. Future exploration should target more complex industry applications, such as intelligent development requirements in finance, healthcare, and manufacturing sectors[10], to validate the tools' universality and robustness.

Third, enhance the precision and reliability of natural language understanding and code generation. Although large models demonstrate strong generalisation capabilities, their accurate comprehension of complex business logic and specialised industry rules requires further refinement. Future efforts should integrate domain knowledge graphs and business rule engines to strengthen models' comprehension of specialised domain knowledge, thereby further improving the accuracy and reliability of generated code.

Fourthly, further enhance debugging efficiency. Combining AI-based debugging tool frameworks with static and dynamic analysis techniques can significantly boost debugging efficiency in complex systems.

Finally, establishing an ecosystem for intelligent development tools. Creating an open marketplace for model services and components will attract more developers to participate in ecosystem development, fostering a virtuous cycle. This will further enrich tool functionality and application scope, promoting the healthy development of intelligent development ecosystems on low-code platforms.

In summary, the integration of large language models with low-code platforms holds vast development

potential. Future research and practice will further advance the maturity and adoption of intelligent development tools, providing more robust technical support for enterprise digital transformation.

REFERENCES

[1] Chen et al. LoRA: Low-Rank Adaptation of Large Language Models ICLR 2024.

[2] Google Research Formal Verification for Generated Code TSE 2025.

[3] China Academy of Information and Communications Technology (CAICT) White Paper on Low-Code Development Platform Security, 2024 Edition.

[4] Liu Yang, Wang Jun. Research on Intelligent Software Development Driven by Large Language Models [J]. Computer Science, 2023, 50(3): 45-52.

[5] Securities Times. 2022 China Low-Code and No-Code Platform Industry Research Report [EB/OL]. PDF document. Available: https://pdf.dfcfw.com/pdf/H3_AP202212061580867579_1.pdf, 2022.

[6] Hinton, G., Vinyals, O., & Dean, J. (2015). Distilling the Knowledge in a Neural Network. arXiv preprint arXiv:1503.02531.

[7] Dosovitskiy, A., Beyer, L., Kolesnikov, A., Weissenborn, D., Zhai, X., Unterthiner, T., et al. (2021). An Image is Worth 16x16 Words: Transformers for Image Recognition at Scale.

[8] Liu, S., & Wang, J. (2023). Gating Mechanisms for Multimodal Large Models.

[9] Felter, W., Ferreira, A., Rajamony, R., & Rubio, J. (2015). An Updated Performance Comparison of Virtual Machines and Linux Containers.

[10] Li, J., Zhang, H., & Wang, Y. (2020). A Survey on Intelligent Software Development Tools: Challenges and Opportunities.

[11] Zhang, X., Li, Y., & Zhao, H. (2019). AI-Powered Debugging: A New Era of Software Development.

[12] He, K., Wang, J., & Zhao, L. (2021). Building an Ecosystem for AI Model Marketplace: Challenges and Opportunities.